

Heat flux and quantum correlations in dissipative cascaded systems

Salvatore Lorenzo,¹ Alessandro Farace,² Francesco Ciccarello,³ G. Massimo Palma,³ and Vittorio Giovannetti²

¹*Dipartimento di Fisica e Chimica, Università degli Studi di Palermo, via Archirafi 36, I-90123 Palermo, Italy*

²*NEST, Scuola Normale Superiore and Istituto Nanoscienze-CNR, I-56126 Pisa, Italy*

³*NEST, Istituto Nanoscienze-CNR and Dipartimento di Fisica e Chimica, Università degli Studi di Palermo, via Archirafi 36, I-90123 Palermo, Italy*

(Dated: August 31, 2018)

We study the dynamics of heat flux in the thermalization process of a pair of identical quantum system that interact dissipatively with a reservoir in a *cascaded* fashion. Despite the open dynamics of the bipartite system S is globally Lindbladian, one of the subsystems “sees” the reservoir in a state modified by the interaction with the other subsystem and hence it undergoes a non-Markovian dynamics. As a consequence, the heat flow exhibits a non-exponential time behaviour which can greatly deviate from the case where each party is independently coupled to the reservoir. We investigate both thermal and correlated initial states of S and show that the presence of correlations at the beginning can considerably affect the heat flux rate. We carry out our study in two paradigmatic cases – a pair of harmonic oscillators with a reservoir of bosonic modes and two qubits with a reservoir of fermionic modes – and compare the corresponding behaviours. In the case of qubits and for initial thermal states, we find that the trace distance discord is at any time interpretable as the correlated contribution to the total heat flux.

PACS numbers: 03.65.Yz,03.67.-a,42.50.Lc,03.65.Ud

I. INTRODUCTION

A fundamental thermodynamic quantity is the amount of energy that can be extracted from non-equilibrium systems. The field of quantum thermodynamics [1–4] is currently experiencing a considerable effort to understand the concepts of work and heat within quantum mechanics [5–10]. While work is commonly analyzed in the presence of external coherent control on the system [3, 4, 6], heat is associated to energy changes that are due to some system-bath interaction [2, 7, 11]. Quantum Thermodynamics tackles heat transfer by modelling the system-bath interactions as a quantum mechanical process mathematically described, under weak-coupling assumptions, by the Lindblad generator [12]. Scenarios featuring consecutive interactions between individual elements of a quantum multipartite system and their own local environments have recently been investigated [13–16] and the study of these correlated channels has made clear that interesting new features emerge in the presence of correlations.

Given the quantum mechanical nature of such processes, an interesting question is if, and how, the heat flux between a multipartite system and its reservoir can be affected by intra-system *quantum* correlations (QCs) which are present in the initial state. In particular, one can investigate whether QCs, either in the form of entanglement [17] or quantum discord [18], are fundamental resources for the heat transfer mechanism. Note that a similar issue was tackled in the completely different framework of quantum biology, see e.g. [19, 20].

It is straightforward to predict that, if the various subsystems are not directly coupled and the reservoir is sufficiently large to prevent any cross-talking, then correlations do not play any role. In such cases, the heat flux emerging from a composite system is the same for all the initial states admitting the same local representation, regardless

of the presence of correlations among its constituents. The scenario however changes drastically if we do introduce interactions among the various subsystems or if the reservoir “sees” the compound systems as a unique object (so called common bath). For instance, it is well known that a strong coupling between two atoms can inhibit energy dissipation via the formation of dark states effectively decoupled from the reservoir [21]. In all these cases, quantum coherence (at the level of either initial correlations or interactions) plays a major role.

In this paper, we shed light on such issues in the case of a cascade bipartite system where energy flows between its subsystems along a specific direction (say from subsystem 1 to subsystem 2 but not the opposite).

Although thermal equilibrium with the heat bath is always reached after an infinite amount of time, a stronger or weaker heat flux can be obtained by engineering correlations in the initial state of the system, giving rise to very different timescales for the thermalization process. This means that the same amount of energy, stored into different configurations of the system, can be retrieved faster or slower according to the chosen state preparation. In our study, we adopt the master equation approach developed by Gardiner *et al.* [22, 23] in the case of bosonic baths and recently generalized by two of us [24] via a collision-model-based approach. Within this framework, we discuss both the case of continuous-variable systems (two quantum harmonic oscillators) and the case of two-level systems (a pair of qubits [25]) showing how the presence of initial correlations can influence the system dynamics by speeding up or slowing down the energy flux to or from the reservoir. Interestingly enough, we find that in both scenarios, while entanglement among the subsystems appears not to play an essential role, the extremal performances in terms of heat flux rate take place in the presence of high values of non-classical correlations [18] in the initial state of the sys-

arXiv:1411.5576v3 [quant-ph] 24 Mar 2015

tem. Yet, strong quantum correlations are not sufficient to ensure faster or slower energy transfer. This is particularly true in the continuous-variable case where states featuring the maximum level of non-classicality do not show any difference in terms of heat fluxes with respect to the completely uncorrelated case. While our analysis is of a conceptual nature (the systems under study being rather idealized) the effects we describe may find potential applications in designing more efficient energy storage units or energy filters.

The outline of the paper is as follows. In Section II, we describe the model under consideration and the master equation describing its open dynamics under a cascade interaction with the reservoir. In Section III, we investigate the general form of the total and local heat fluxes and show that the former can be decomposed into three contributions, one of which reflects the interaction between the subsystems mediated by the reservoir. In Section IV, we address the general time dependence of heat fluxes for both harmonic oscillators and qubits. In Section V, (case of harmonic oscillators) and VI (qubits) we analyze extensively the heat flux dynamics when the initial state of the open system is thermal or correlated (but locally thermal). We furthermore investigate on the role of initial QCs. In Section VII, we show that in some cases the correlated heat flux can be directly connected to a discord-like measure of QCs. Finally, in Section VIII, we draw our conclusions.

II. MODEL AND MASTER EQUATION

We consider a bipartite open system S , consisting of a pair of subsystems S_1 and S_2 , and a thermal reservoir R modeled as a large ensemble of identical ancillas all in the same initial thermal state. The S - R interaction occurs in *cascade* [26]. S_1 interacts with R through a sequence of system-ancilla collisions under the usual Born-Markov approximation [27]. S_2 , instead, interacts with R *modified* by the previous interaction with S_1 , see Fig. 1(a). No direct mutual coupling between S_1 and S_2 is present. Yet, R mediates an indirect coupling between them. Such indirect S_1 - S_2 coupling is however *unidirectional*: S_1 affects the dynamics of S_2 , but S_2 cannot influence S_1 in any way. The master equation in the S state ρ at time t was derived long ago for bosonic baths through the input-output formalism [22, 23, 28] and, quite recently, generalized to arbitrary baths by means of a collision-model-based approach [24]. To simplify the analysis, in what follows we shall assume that the delay time between the S_1 - R and S_2 - R collisions is negligible compared to all the other system time scales. Still, the causal structure of the process holds: a collision between S_1 and a given ancilla of R will anyway occur *before* the latter collides with S_2 , see Fig. 1(a). Accordingly the master equation is of the Kossakowski-Lindblad form [27] and reads

$$\dot{\rho} = -\frac{i}{\hbar}[\hat{H}, \rho] + \mathcal{L}^{(c)}(\rho), \quad (1)$$

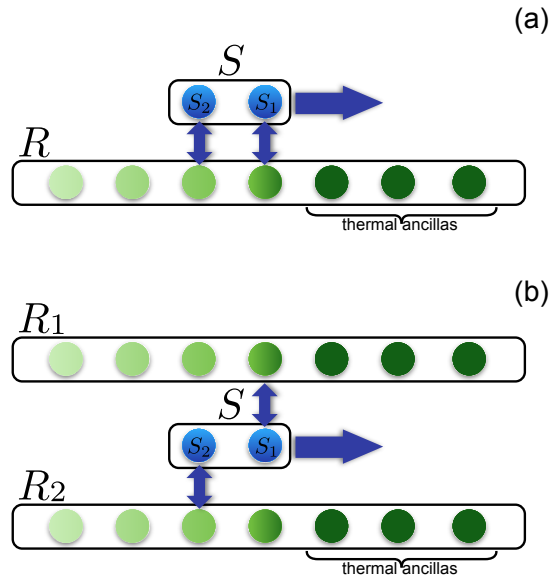


Figure 1. (Color online)(a) Sketch of the cascade interaction between S and R . In this collision-model-based picture, R is modelled as a large collection of ancillas. Each subpart S_i of system S interacts in succession with the reservoir ancillas. S_1 always interacts with ancillas that are in a thermal state. In contrast, S_2 encounters ancillas that have previously interacted with S_1 (hence they are no more in thermal state). For the sake of simplicity in our analysis the delay time which elapses between the collision of a given ancilla elements with S_1 and the subsequent collision with S_2 is assumed to be negligible with respect to the other time scales of the system (see main text). (b) Sketch of the model where the cascade interaction has been removed. In this case the evolution of S_1 and S_2 is the same as if they were interacting with two copies (R_1 and R_2) of the same reservoir.

where $\hat{H} = \hat{H}_1 + \hat{H}_2$ is the free Hamiltonian of S (\hat{H}_i is the local free Hamiltonian of the i th subsystem with $i = 1, 2$) while the cascade Lindbladian superoperator $\mathcal{L}^{(c)}$ is the sum of three terms according to

$$\mathcal{L}^{(c)} = \mathcal{L}_1 + \mathcal{L}_2 + \mathcal{D}_{12}. \quad (2)$$

Here, \mathcal{L}_i acts locally on S_i only and coincides with the Lindblad superoperator that would be obtained if S_i were in contact with R in the absence of the other subsystem. The superoperator \mathcal{D}_{12} , instead, acts on both the subsystems and accounts for the cascade, i.e., one-way, $S_1 \rightarrow S_2$ interaction mediated by R . The explicit forms of \mathcal{L}_i and \mathcal{D}_{12} will be given below in the cases of concern to this work (for simplicity, we will refer to such superoperators as “dissipators” since we will focus on purely dissipative

reservoirs). The general expressions for $\{\mathcal{L}_i\}$ and \mathcal{D}_{12} can be found in [24]. For comparison, we will also analyze the case where the cascade link is removed in a way that both systems interact with the reservoir R independently, see Fig. 1(b). Formally, this can be obtained by simply replacing in Eq. (1) $\mathcal{L}^{(c)}$ with $\mathcal{L}^{(ind)} = \mathcal{L}_1 + \mathcal{L}_2$ (i.e., by setting $\mathcal{D}_{12} = 0$).

We next illustrate the explicit form taken by \mathcal{L}_i and \mathcal{D}_{12} for a pair of CV variables (i.e., quantum harmonic oscillators) and qubits (i.e., two-level systems) in contact with a reservoir of harmonic oscillators and qubits, respectively.

A. Harmonic oscillators

In this case, each subsystem S_i is a quantum harmonic oscillator of frequency ω with associated bosonic annihilation and creation operators \hat{a}_i and \hat{a}_i^\dagger , respectively. The free Hamiltonian reads

$$\hat{H} = \hat{H}_1 + \hat{H}_2 = \hbar\omega(\hat{a}_1^\dagger\hat{a}_1 + \hat{a}_2^\dagger\hat{a}_2). \quad (3)$$

The reservoir R consists of a large collection of bosonic modes. If the interaction Hamiltonian between the system and each reservoir mode does not feature counter-rotating terms (rotating-wave approximation), the local and non-local dissipators in Eq.(2) are then given by [23, 24]

$$\begin{aligned} \mathcal{L}_i(\rho) = & \frac{\gamma}{2}(N+1) \left(2\hat{a}_i\rho\hat{a}_i^\dagger - \rho\hat{a}_i^\dagger\hat{a}_i - \hat{a}_i^\dagger\hat{a}_i\rho \right) \\ & + \frac{\gamma}{2}N \left(2\hat{a}_i^\dagger\rho\hat{a}_i - \rho\hat{a}_i\hat{a}_i^\dagger - \hat{a}_i\hat{a}_i^\dagger\rho \right), \end{aligned} \quad (4)$$

$$\begin{aligned} \mathcal{D}_{12}(\rho) = & \gamma(N+1) \left(\hat{a}_1[\rho, \hat{a}_2^\dagger] + [\hat{a}_2, \rho]\hat{a}_1^\dagger \right) \\ & + \gamma N \left(\hat{a}_1^\dagger[\rho, \hat{a}_2] + [\hat{a}_2^\dagger, \rho]\hat{a}_1 \right). \end{aligned} \quad (5)$$

Here, γ coincides with the relaxation rate that would arise for each subsystem alone (assumed identical for the two subsystems), $N = 1/(e^{\beta\hbar\omega} - 1)$ is the thermal excitation number, $\beta = 1/(k_B T)$ is the inverse temperature, while k_B and T are the Boltzmann constant and reservoir's temperature, respectively.

B. Qubits

In this case, each subsystem S_i is a two-level system (qubit) whose ground and excited states are $|g\rangle_i$ and $|e\rangle_i$, respectively. The corresponding energy gap is $\hbar\omega$. Let $\{\hat{\sigma}_{i\pm}, \hat{\sigma}_{iz}\}$ be the usual pseudo-spin operators with $\hat{\sigma}_{i+} = \hat{\sigma}_{i-}^\dagger = |e\rangle_i\langle g|$ and $\hat{\sigma}_{iz} = |e\rangle_i\langle e| - |g\rangle_i\langle g|$. The system's free Hamiltonian now reads

$$\hat{H} = \hat{H}_1 + \hat{H}_2 = \frac{\hbar\omega}{2} (\hat{\sigma}_{1z} + \hat{\sigma}_{2z}). \quad (6)$$

If the reservoir consists of a bath of qubits, under the rotating-wave approximation the local and non-local dissi-

pators in Eq.(2) are given by [24]

$$\begin{aligned} \mathcal{L}_i = & \frac{\gamma}{4}(1+\xi) (2\hat{\sigma}_{i-}\rho\hat{\sigma}_{i+} - \rho\hat{\sigma}_{i+}\hat{\sigma}_{i-} - \hat{\sigma}_{i+}\hat{\sigma}_{i-}\rho) \\ & + \frac{\gamma}{4}(1-\xi) (2\hat{\sigma}_{i+}\rho\hat{\sigma}_{i-} - \rho\hat{\sigma}_{i-}\hat{\sigma}_{i+} - \hat{\sigma}_{i-}\hat{\sigma}_{i+}\rho), \end{aligned} \quad (7)$$

$$\begin{aligned} \mathcal{D}_{12} = & \frac{\gamma}{2}(1+\xi) (\hat{\sigma}_{1-}[\rho, \hat{\sigma}_{2+}] + [\hat{\sigma}_{2-}, \rho]\hat{\sigma}_{1+}) \\ & + \frac{\gamma}{2}(1-\xi) (\hat{\sigma}_{1+}[\rho, \hat{\sigma}_{2-}] + [\hat{\sigma}_{2+}, \rho]\hat{\sigma}_{1-}) \end{aligned} \quad (8)$$

with

$$\xi = \tanh \left[\frac{\hbar\omega/2}{k_B T} \right]. \quad (9)$$

Note that Eqs. (7) and (8) have the same structure as Eqs. (4) and (5), but differ from these in the statistical nature of ladder operators (fermionic instead of bosonic) and the rates associated with the dissipators.

III. TOTAL AND LOCAL HEAT FLUXES

Both in the case of harmonic oscillators and qubits, any initial state $\rho(0)$ of the system asymptotically relaxes towards the stationary state

$$\rho(\infty) = \frac{e^{-\beta\hat{H}_1}}{Z} \otimes \frac{e^{-\beta\hat{H}_2}}{Z} \quad (10)$$

with $Z = \text{Tr}_i[e^{-\beta\hat{H}_i}]$ (since the subsystems are identical, Z does not depend on $i=1,2$). This can be checked by setting $\dot{\rho} = 0$ in Eq. (1) and verifying that the resulting equation is fulfilled by state (10), as proven in detail in Appendix A for both harmonic oscillators and qubits. Eq. (10) shows that the system thermalizes to the reservoir temperature. The asymptotic thermal state coincides with the one that would be obtained if S_1 and S_2 were in contact with R independently [i.e., $\rho(\infty)$ is also the fixed point associated with the dissipator $\mathcal{L}^{(ind)}$]. Thereby, the presence of the correlated dissipator \mathcal{D}_{12} in Eq. (1) has no effect on the steady state, which is indeed fully factorized and does not feature any S_1 - S_2 correlation, nor on the total amount of energy which is exchanged with the reservoir, i.e.,

$$Q(\infty) = \text{Tr}[(\rho(\infty) - \rho(0))\hat{H}]. \quad (11)$$

However, significant correlations can in general arise during the *transient*. In turn, these correlations affect the way heat flows between S – specifically S_2 – and R . The heat flux dynamics during such transient will be the focus of our analysis.

As in our model no external work is done on S , the *total* heat flux of S – we call it J – can be identified with the time derivative of the system energy $U = \text{Tr}[\rho\hat{H}]$ [11]. Hence, at time t , the heat flux is calculated as $J(t) = \dot{U} = \text{Tr}[\dot{\rho}(t)\hat{H}]$. In the case of the cascaded system, due to Eqs. (1) and (2), this yields

$$J^{(c)}(t) = \mathcal{J}_1(t) + \mathcal{J}_2(t) + \mathcal{J}_{12}(t) \quad (12)$$

with

$$\mathcal{J}_i(t) = \text{Tr} \left[\mathcal{L}_i \rho(t) \hat{H} \right] \equiv \text{Tr} \left[\mathcal{L}_i \rho(t) \hat{H}_i \right], \quad (13)$$

$$\mathcal{J}_{12}(t) = \text{Tr} \left[\mathcal{D}_{12} \rho(t) \hat{H} \right] \equiv \text{Tr} \left[\mathcal{D}_{12} \rho(t) \hat{H}_2 \right]. \quad (14)$$

The total heat flux can thus be decomposed into three contributions, two of which stem from the local dissipators $\{\mathcal{L}_i\}$, one from the non-local dissipator \mathcal{D}_{12} . In Eqs. (13) and (14), the last identities show that \hat{H} can be replaced by \hat{H}_i (\hat{H}_2) in the calculation of \mathcal{J}_i (\mathcal{D}_{12}). This is due to the identities

$$\text{Tr}[\mathcal{L}_1 \rho \hat{H}_2] = \text{Tr}[\mathcal{L}_2 \rho \hat{H}_1] = \text{Tr}[\mathcal{D}_{12} \rho \hat{H}_1] = 0, \quad (15)$$

which can be straightforwardly proven upon use of Eqs. (4) and (7) and the cyclic property of the trace.

As for the *local* heat fluxes of S_1 and S_2 , by using Eqs. (1), (2), (13)-(15) these are respectively computed as

$$J_1^{(c)}(t) = \dot{U}_1(t) = \text{Tr} \left[\dot{\rho}(t) \hat{H}_1 \right] \equiv \mathcal{J}_1(t), \quad (16)$$

$$J_2^{(c)}(t) = \dot{U}_2(t) = \text{Tr} \left[\dot{\rho}(t) \hat{H}_2 \right] \equiv \mathcal{J}_2(t) + \mathcal{J}_{12}(t). \quad (17)$$

Upon comparison of these with the total heat flux (12), we find $J^{(c)}(t) = J_1^{(c)}(t) + J_2^{(c)}(t)$ as expected. More importantly, the above equations show that, out of the three terms appearing in Eq. (12), $\mathcal{J}_1(t)$ accounts for the S_1 heat flux while the sum of the last two, i.e., $\mathcal{J}_2(t) + \mathcal{J}_{12}(t)$, is equal to $J_2^{(c)}(t)$. The correlated term $\mathcal{J}_{12}(t)$ therefore contributes only to the heat flux of S_2 (this is reasonable in light of the cascaded nature of the system dynamics). As anticipated, the reduced dynamics of S_1 fully coincides with that in the absence of S_2 since, upon trace over subsystem S_2 and using the cyclic property of the partial trace, Eq. (1) yields $\dot{\rho}_1 = \mathcal{L}_1 \rho_1$. Correspondingly, $J_1^{(c)}(t)$ is just the same function as in the absence of S_2 since in Eq. (16) $\rho(t)$ can be replaced with $\rho_1(t)$.

The heat flux associated with the identical and independent reservoirs model of Fig.1(b) can be calculated in the same way. Again the total flux is given by the sum of the fluxes from S_1 and from S_2 , i.e. $J^{(ind)}(t) = J_1^{(ind)}(t) + J_2^{(ind)}(t)$. Furthermore the heat flux $J_1^{(ind)}(t)$ from S_1 coincides with the one we computed for the cascaded system, i.e., $J_1^{(ind)}(t) = J^{(c)}(t) = \mathcal{J}_1(t)$, hence the two models give rise to the same reduced local dynamics for S_1 . On the contrary the heat flux from S_2 , $J_2^{(ind)}(t)$ is rather different from $J_2^{(c)}(t)$. In particular, if we do assume that the initial state $\rho(0)$ is locally indistinguishable for exchange of S_1 with S_2 , we have $J_2^{(ind)}(t) = J_1^{(ind)}(t) = \mathcal{J}_1(t)$ (the local dissipative processes being identical). Accordingly, we can write

$$J^{(ind)}(t) = 2\mathcal{J}_1(t), \quad (18)$$

with $\mathcal{J}_1(t)$ being the *same* function that appears on the right-hand-side of Eq. (12). It is finally worth stressing that due to the fact that both the cascade and the independent

model yield the same total amount of dissipated energy (11) when integrated over the whole evolution [i.e., $Q(\infty) = \int_0^\infty J^{(c)}(t) dt = \int_0^\infty J^{(ind)}(t) dt$], the following identity holds

$$\int_0^\infty [\mathcal{J}_1(t) - \mathcal{J}_2(t)] dt = \int_0^\infty \mathcal{J}_{12}(t) dt. \quad (19)$$

IV. TIME DEPENDANCE OF HEAT FLUXES

In this section, we show how the explicit procedure to calculate the three contributions to the total heat flux of Eq. (2), for harmonic oscillators and for qubits.

A. Harmonic oscillators

In the case of harmonic oscillators, we focus on initial states $\rho(0)$ of S that are *Gaussian* [29]. The linearity of the master equation (1) alongside the assumption that the initial state of the ancillas of R is thermal (hence Gaussian as well) ensures that the state of S will remain Gaussian at any time t . To specify such states, let us introduce the position-momentum quadrature operators $\hat{X}_j = (\hat{a}_j^\dagger + \hat{a}_j)/\sqrt{2}$ and $\hat{Y}_j = i(\hat{a}_j^\dagger - \hat{a}_j)/\sqrt{2}$ with $j=1, 2$. Correspondingly, let us define the four-dimensional vector operator $\hat{\chi} = \{\hat{X}_1, \hat{Y}_1, \hat{X}_2, \hat{Y}_2\}$. By definition, a Gaussian state is fully specified by the expectation value of $\hat{\chi}$, i.e., $\{\langle \hat{X}_j \rangle, \langle \hat{Y}_j \rangle\}$, and by the covariance matrix $C_{mn} = \langle \frac{1}{2}(\hat{\chi}_m \hat{\chi}_n + \hat{\chi}_n \hat{\chi}_m) \rangle - \langle \hat{\chi}_m \rangle \langle \hat{\chi}_n \rangle$ with $m, n=1, \dots, 4$. Throughout, we will consider states with vanishing first moments, i.e., $\langle \hat{\chi}(0) \rangle = 0$, which amounts to assuming that the energy of S is initially stored solely in the form of fluctuations. Indeed, correlations are entirely described by the fluctuations and our main concern is to highlight the interplay between heat fluxes and correlations. Each initial state we will consider, thereby, will be fully specified by the covariance matrix C_{mn} (this has real entries).

For the class of initial states discussed so far, upon use of Eqs. (4), (5), (13) and (14) the three heat fluxes on the right-hand side of Eq. (12) take the form

$$\mathcal{J}_1(t) = \hbar\omega\gamma \left[\frac{C_{11}(t) + C_{22}(t)}{2} - \left(N + \frac{1}{2}\right) \right], \quad (20)$$

$$\mathcal{J}_2(t) = \hbar\omega\gamma \left[\frac{C_{33}(t) + C_{44}(t)}{2} - \left(N + \frac{1}{2}\right) \right], \quad (21)$$

$$\mathcal{J}_{12}(t) = \hbar\omega\gamma [C_{13}(t) + C_{24}(t)]. \quad (22)$$

To calculate the explicit time evolution of the covariance matrix entries $C_{mn}(t)$ for a given initial state, it is convenient to use the Langevin equations [23] as illustrated in Appendix B

B. Qubits

In this case, with the help of Eqs. (7), (8), (13) and (14) the contributions to the total heat flux on the right-hand

side of Eq. (12) are calculated as

$$\mathcal{J}_1(t) = \gamma \left[(1+\xi)[\rho_{11}(t) + \rho_{22}(t)] - (1-\xi)[\rho_{33}(t) + \rho_{44}(t)] \right], \quad (23)$$

$$\mathcal{J}_2(t) = \gamma \left[(1+\xi)[\rho_{11}(t) + \rho_{33}(t)] - (1-\xi)[\rho_{22}(t) + \rho_{44}(t)] \right], \quad (24)$$

$$\mathcal{J}_{12}(t) = 2\gamma\xi [\rho_{23}(t) + \rho_{32}(t)], \quad (25)$$

where ρ_{mn} , i.e., the matrix elements of ρ , are labeled according to the uncoupled basis of the S Hilbert space $\{|ee\rangle_{12}, |eg\rangle_{12}, |ge\rangle_{12}, |gg\rangle_{12}\}$. Eqs. (23)-(25) hold for an arbitrary initial two-qubit state $\rho(0)$. To calculate the explicit time evolution of the density matrix entries $\rho_{mn}(t)$ for a given $\rho(0)$, it is convenient to use master equation (1) in the Liouville space as shown in Appendix C.

V. HEAT FLUX DYNAMICS: HARMONIC OSCILLATORS

In this section, we analyse the heat flux dynamics for a pair of harmonic oscillators. We will consider both thermal (hence uncorrelated) and correlated initial states of the reservoir.

A. Thermal initial states

In this case, the pair of harmonic oscillators S is initially in a thermal state $\rho(0) = e^{-\beta_S \hat{H}_1} \otimes e^{-\beta_S \hat{H}_2} / Z_S^2$, where $Z_S = \text{Tr}_i[e^{-\beta_S \hat{H}_i}]$, $\beta_S = 1/(k_B T_S)$ and T_S is the system initial temperature. Note that, due to the lack of a direct coupling between S_1 and S_2 , in such situation the two subsystems are initially fully *uncorrelated* and identical under mutual exchange. Such initial conditions correspond to a covariance matrix whose only non-zero entries are $C_{ii}(0) = N_S + 1/2$ for any $i=1, \dots, 4$. Here, $N_S = 1/(e^{\beta_S \hbar \omega} - 1)$ is the initial average number of excitations in either S 's subsystem, which in general differs from N (average number of excitations at the reservoir temperature). With the help of Eqs. (20)-(22) and Appendix B, the explicit time dependences of \mathcal{J}_1 , \mathcal{J}_2 and \mathcal{J}_{12} is shown to be

$$\mathcal{J}_1(t) = \hbar\omega\gamma(N_S - N)e^{-\gamma t}, \quad (26)$$

$$\mathcal{J}_2(t) = (1 + \gamma^2 t^2)\mathcal{J}_1(t), \quad \mathcal{J}_{12}(t) = -2\gamma t \mathcal{J}_1(t), \quad (27)$$

and hence the heat flux of S_2 [cf. Eq. (17)] for the cascade model reads

$$J_2^{(c)}(t) = (1 - \gamma t)^2 \mathcal{J}_1(t), \quad (28)$$

so that

$$\begin{aligned} J^{(c)}(t) &= [1 + (1 - \gamma t)^2] \mathcal{J}_1(t) \\ &= \hbar\omega\gamma(N_S - N) [1 + (1 - \gamma t)^2] e^{-\gamma t}, \end{aligned} \quad (29)$$

In Fig. 2 (first column), we plot $J^{(c)}(t)$ and its three components $\{\mathcal{J}_1(t), \mathcal{J}_2(t), \mathcal{J}_{12}(t)\}$ for different values of T_S both above and below the reservoir's temperature T which is chosen to be comparable with the typical energy scale of the system (specifically we assume $k_B T / (\hbar\omega) = 1$). As

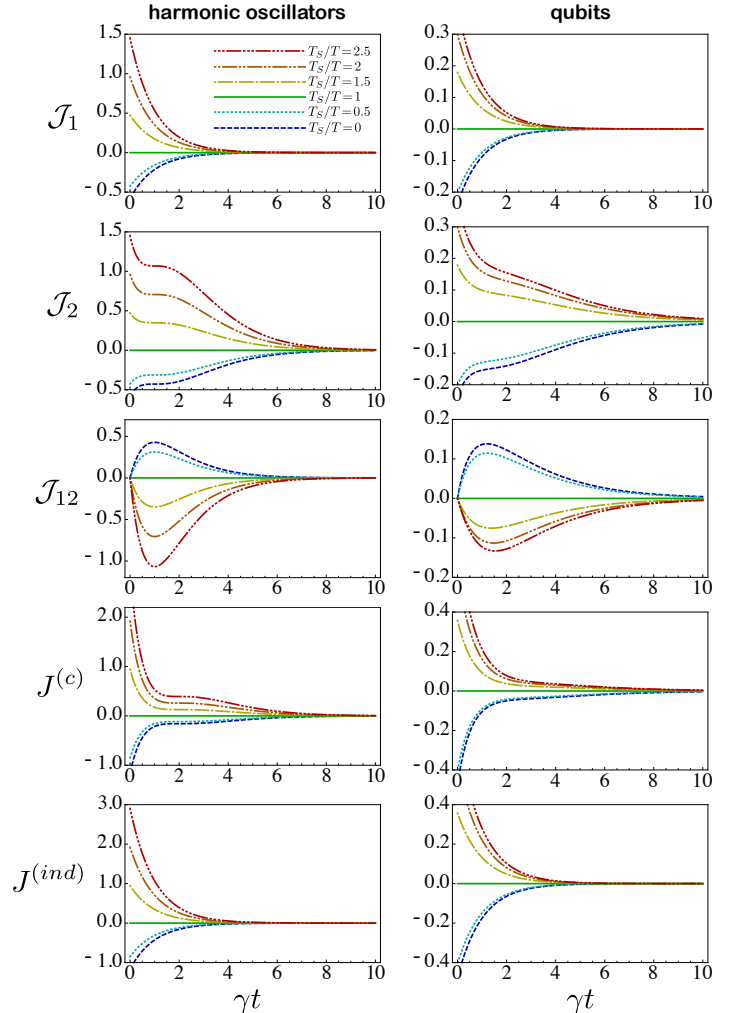


Figure 2. (Color online) Heat flows \mathcal{J}_1 , \mathcal{J}_2 , \mathcal{J}_{12} and total heat flow $J^{(c)}$ against time in the case of harmonic oscillators (left-column plots) and qubits (right-column plots) for various temperatures T_S (see the colour legend in the topmost left figure). As for the reservoir temperature, we have set it in such a way to have $k_B T / (\hbar\omega) = 1$. Heat flows are expressed in unit of $\hbar\omega\gamma$ and time is expressed in units of γ^{-1} . In the bottom plots, we also report the behaviour of $J^{(ind)}$ for comparison.

expected, the heat flux of S_1 exponentially decays or increases [depending on the sign of $(N_S - N)$] at the rate γ . In contrast, both $\mathcal{J}_2(t)$ and $\mathcal{J}_{12}(t)$ exhibit non-exponential behaviour. The correlated heat $\mathcal{J}_{12}(t)$, in particular, has a non-monotonic behaviour: its absolute value grows from zero until it reaches a maximum at $\gamma t = 1$ and then decreases. Also, note that the sign of $\mathcal{J}_{12}(t)$ is always opposite to that of $\mathcal{J}_1(t)$. The non-monotonic behaviour of $\mathcal{J}_2^{(c)}(t)$ affects the total heat flow $J^{(c)}(t)$ to a significant extent. To better appreciate this consider the scenario in which S_1 and S_2 are fully independent. The total flux in this case is expressed by Eq. (18), i.e.

$$J^{(ind)}(t) = 2\mathcal{J}_1(t) = 2 \hbar\omega\gamma(N_S - N) e^{-\gamma t}. \quad (30)$$

By a direct comparison with Eq. (29) it follows that the cascading mechanism makes $|J^{(c)}|$ lower (higher) than $|J^{(ind)}|$ for times shorter (larger) than $\gamma t = 2$ (while maintaining the same sign in any case). In particular for $T_S > T$ this implies that, when connected in cascade, S_1 and S_2 tend to retain energy for a longer time.

B. Correlated initial states

Next, we investigate the effect of initial correlations between S_1 and S_2 on the heat flux dynamics. Specifically, we consider initial states $\rho(0)$ such that $\rho_1(0) = \text{Tr}_2[\rho(0)] = e^{-\beta_S \hat{H}_1} / Z_S$ and $\rho_2(0) = \text{Tr}_1[\rho(0)] = e^{-\beta_S \hat{H}_2} / Z_S$ but $\rho(0) \neq \rho_1(0) \otimes \rho_2(0)$. In other words, one such state is *locally* equivalent to a tensor product of thermal states at the same temperature T_S (like those addressed in Subsection V A) but we allow S_1 and S_2 to initially share some correlations. For the sake of simplicity, we will focus on the case where the reservoir is at zero temperature, i.e., we set $N=0$ throughout.

In line with Subsection V A, the requirement that the state is locally thermal at the uniform temperature T_S (corresponding to the average excitation number N_S) yields that the diagonal entries of the initial-state covariance matrix are $C_{ii}(0) = N_S + 1/2$ for any $i = 1, \dots, 4$. The energy is then given by $U = \frac{1}{2} \hbar \omega \text{Tr}[C(0)] = 2 \hbar \omega C_{11}(0)$. The remaining entries of $C(0)$ are set to zero except for $C_{13}(0) = C_{31}(0)$ and $C_{24}(0) = C_{42}(0)$ that can be non-null. This is because, at an arbitrary time t , the only off-diagonal entries which the heat fluxes depend on are $C_{13}(t)$ and $C_{24}(t)$ [cf. Eq. (22)]. Moreover, as shown by Eqs. (B8) and (B9) in Appendix B, the initial values of the remaining off-diagonal elements do not affect the heat-flux dynamics since these are fully decoupled from $\{C_{13}(t), C_{24}(t)\}$. To summarise, we study initial states having the form

$$C(0) = \begin{pmatrix} C_{11}(0) & 0 & C_{13}(0) & 0 \\ 0 & C_{11}(0) & 0 & C_{24}(0) \\ C_{13}(0) & 0 & C_{11}(0) & 0 \\ 0 & C_{24}(0) & 0 & C_{11}(0) \end{pmatrix}. \quad (31)$$

A rigorous parametrization of the family of covariance matrices of the form (31) is presented in Appendix D.

Clearly, the heat flux of S_1 is again given by Eq. (26) with $N=0$. This immediately implies that the total flux $J^{(ind)}(t)$ for the independent system model remains identical to the one computed in Eq. (30), and will not depend upon the presence of initial correlations. On the contrary with the help of Eqs. (20)-(22) and Appendix B the two contributions to the S_2 heat flux for the cascade system are calculated as

$$\mathcal{J}_2(t) = (1 + \gamma^2 t^2) \mathcal{J}_1(t) - \hbar \omega \gamma t [C_{13}(0) + C_{24}(0)] e^{-\gamma t}, \quad (32)$$

$$\mathcal{J}_{12}(t) = -2\gamma t \mathcal{J}_1(t) + \hbar \omega \gamma [C_{13}(0) + C_{24}(0)] e^{-\gamma t}. \quad (33)$$

Upon sum of these we thus obtain

$$J_2^{(c)}(t) = (1 - \gamma t)^2 \mathcal{J}_1(t) + \hbar \omega \gamma (1 - \gamma t) [C_{13}(0) + C_{24}(0)] e^{-\gamma t}. \quad (34)$$

Eqs. (32)-(34) generalize Eqs. (27)-(28), featuring additional terms proportional to $C_{13}(0) + C_{24}(0)$. Importantly, the fact that the heat flux depends on such off-diagonal entries only through their *sum* entails that for states such that $C_{13}(0) = -C_{24}(0)$, irrespective of $|C_{13}(0)|$, the presence of initial correlations has no effect on the heat flux dynamics.

To illustrate the typical behavior of the total heat flux in the general case, in figure 3(a) we plot the total flux $J^{(c)}(t)$ of Eq. (12) for $N_S = 1$ and $C_{13}(0) = C_{24}(0) = -0.7N_S, 0, 0.7N_S$. We point out that, as explained in Appendix D, focusing on states such that $C_{13}(0) = C_{24}(0)$ does not cause loss of generality. As shown by the plots, in contrast to figure 2, a major consequence of the presence of initial correlations is the non-monotonicity of the heat flux time. This can be proven in detail through a study of the derivative of $J^{(c)}(t)$, as resulting from the sum of Eqs. (26) and (34).

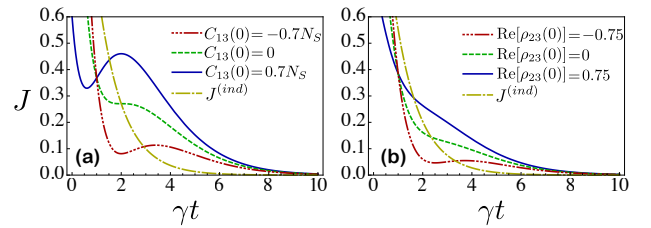


Figure 3. (Color online) (a): Time evolution of the total heat flux $J^{(c)}(t) = J_1^{(c)}(t) + J_2^{(c)}(t)$ for the cascade model in the case of harmonic oscillators for different choices of $C_{13}(0) = C_{24}(0)$, where we have set $N_S = 1$ and $N = 0$. (b): Time evolution of the total heat flux in the case of qubits for different choices of $\text{Re}[\rho_{23}(0)]$, where we have set $\xi_S = 0.25$ and $\xi = 1$. In both cases, heat fluxes are in units of $\hbar \omega \gamma$ and time is in units of γ^{-1} . For comparison, the behaviour of J^{ind} is also reported, which is independent of C_{13} ($\text{Re}[\rho_{23}(0)]$) for harmonic oscillators (qubits).

The derivative reads

$$J^{(c)}(t) = \hbar \omega \gamma^2 \{ -(\gamma^2 N_S) t^2 + \{ \gamma [C_{13}(0) + C_{24}(0) + 4N_S] \} t - 2[C_{13}(0) + C_{24}(0) + 2N_S] \} e^{-\gamma t}.$$

As shown in Appendix D, $|C_{13}(0) + C_{24}(0)| \leq 2N_S$. Hence, in the above equation, the concave-down parabolic time function between curly brackets is non-positive at $t = 0$. Moreover, this function has the two positive real roots

$$t_1 = \frac{2}{\gamma}, \quad t_2 = \frac{2}{\gamma} \left[1 + \frac{C_{13}(0) + C_{24}(0)}{2N_S} \right]. \quad (35)$$

Thereby, $J^{(c)}(t)$ always exhibits a local minimum followed by a local maximum. Specifically, if $[C_{13}(0) + C_{24}(0)] \leq 0$ the minimum occurs at t_2 and the maximum at $t_1 > t_2$. Conversely, if $[C_{13}(0) + C_{24}(0)] > 0$ the minimum occurs at t_1 and the maximum at $t_2 > t_1$. Such stationary points merge into a single inflection point, thus giving rise to a monotonic $J^{(c)}(t)$, for $C_{13}(0) + C_{24}(0) = 0$.

Remarkably, not only the magnitude but even the sign of $C_{13}(0) + C_{24}(0)$ affects the heat flux in a significant way.

This can be appreciated in figure 3(a), which shows that the energy flow of S into the reservoir proceeds slower when $C_{13}(0)+C_{24}(0)<0$. When the sum is positive, in contrast, most of the energy is released in the early stages of the dynamics. Such different behaviours can be better understood by calculating the value of $J^{(c)}(t)$ at $t=0$ and at times $t_{1,2}$ given by (35), which yields

$$J^{(c)}(0) = \hbar\omega\gamma[2N_S + C_{13}(0) + C_{24}(0)], \quad (36)$$

$$J^{(c)}(t_1) = \hbar\omega\gamma\{2N_S - [C_{13}(0) + C_{24}(0)]\}e^{-2}, \quad (37)$$

$$J^{(c)}(t_2) = \hbar\omega\gamma[2N_S + C_{13}(0) + C_{24}(0)]e^{-\frac{[2N_S + C_{13}(0) + C_{24}(0)]}{N_S}}. \quad (38)$$

Hence, if $C_{13}(0)+C_{24}(0)$ is positive, the first minimum always occurs at time t_1 and equals $J^{(c)}(t_1)$. As $e^{-2} \simeq 0.135$ [cf. Eq. (37)], in this case a drop of the heat flux of at least $\simeq 86\%$ takes place after a time $2/\gamma$. The following rise of $J^{(c)}(t)$ is modest given that also the local maximum $J^{(c)}(t_2)$ is at most $\simeq 14\%$ of the initial heat flux. Quite differently, if $C_{13}(0)+C_{24}(0)$ is negative, the minimum occurs at time t_2 , hence the corresponding drop amounts to the exponential factor in Eq. (38) which does not exceed $\simeq 86\%$, this bound occurring in the limiting case of very small $C_{13}(0)+C_{24}(0)$. As this grows, the exponential factor rapidly approaches 1 (correspondingly the drop becomes less and less significant).

To characterise the release time of the system energy in more quantitative terms, in figure 4(a) we analyze $\gamma\tau_p$, namely the time (in units of γ^{-1}) taken by a certain percentage $p\%$ of the initial energy of S to be lost into the reservoir. That is, we compute the energy lost up to some time t as $Q^{(c)}(t) \equiv \int_0^t J^{(c)}(t')dt'$ and we search for the time τ_p at which $Q^{(c)}(\tau_p) = p\% Q^{(c)}(\infty)$ (i.e., $p\%$ of the total transferred energy). In figure 4(a), we plot $\gamma\tau_p$ versus $C_{13}(0)+C_{24}(0)$ for different values of the percentage p (the outcomes are independent of N_S). The plots show that positive (negative) values of $C_{13}(0)+C_{24}(0)$ always speed up (slow down) the energy release compared to the uncorrelated case.

C. Influence of initial quantum correlations

Next, we investigate the role played by typical measures of initial quantum correlations possessed by a state of the form (31). Traditionally, QCs have been associated with *entanglement* [17]. More recently, however, a new paradigm of QCs – associated with the so called *quantum discord* – has been put forward [18]. The need for introducing such a new type of QCs relies on the observation that, although separable, some bipartite states can feature correlations that are incompatible with classical physics. Specifically, here we will use logarithmic negativity [31] (E_N) and Gaussian discord [32] (D_G) in order to quantify entanglement and discord-like QCs, respectively. Details on both measures can be found in Appendix F. Figures 5 shows density plots of logarithmic negativity (a) and Gaussian discord (b) on the $C_{13}(0) - C_{24}(0)$ plane for $N_S = 1$ and $N = 0$

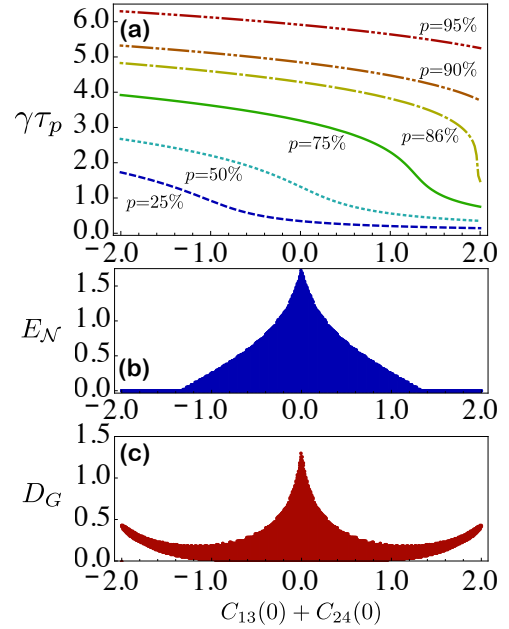


Figure 4. (Color online) (a): $\gamma\tau_p$ against $C_{13}(0)+C_{24}(0)$ for $p=95$ (red three-dotted-dashed line), $p=90$ (orange two-dotted-dashed), $p=86$ (yellow dot-dashed), $p=75$ (green solid), $p=50$ (cyan dotted) and $p=25$ (blue dashed). (b): Entanglement, as measured by the logarithmic negativity E_N , for all the states having the same value of $C_{13}(0)+C_{24}(0)$ as a function of $C_{13}(0)+C_{24}(0)$. (c): Gaussian discord D_G for all the states having the same value of $C_{13}(0)+C_{24}(0)$ as a function of $C_{13}(0)+C_{24}(0)$. Throughout, we have set $N_S=1$ and $N=0$.

(i.e., the paradigmatic instance addressed in the previous subsection). Entanglement E_N arises only in two small regions next to the points $C_{13}(0) = -C_{24}(0) = \sqrt{N_S(N_S+1)}$ and $C_{13}(0) = -C_{24}(0) = -\sqrt{N_S(N_S+1)}$ [33]. In both cases, the corresponding state is close to an EPR state [34]. Instead, Gaussian discord D_G is zero only at the point $C_{13}(0) = C_{24}(0) = 0$, which corresponds to a fully uncorrelated product state. It grows when the distance from this point increases. The steepest-increase directions are given by $C_{13}(0) = -C_{24}(0)$ (where also E_N increases) and $C_{13}(0) = C_{24}(0)$ (where instead entanglement is fully absent).

As discussed in the previous subsection (see also Appendix D), for any possible choice of $C_{13}(0) = C_{24}(0) = c_0$ there is a class of equivalent states (identified by $C_{13}(0)+C_{24}(0) = 2c_0$) which exhibit the same heat flux dynamics [cf. Eqs. (32) and (33)]. The union of these classes coincides with the whole set of physical initial states. As shown in figure 5, all the states in a given class feature non-null D_G [except for $C_{13}(0) = C_{24}(0) = 0$], while a relevant fraction of them not entangled. In figures 4(b) and (c), for each value of $C_{13}(0)+C_{24}(0)$, we report all the possible values of E_N and D_G in the corresponding equivalence class. We see that the states giving rise to the fastest and slowest energy release [corresponding to the highest and lowest values of $C_{13}(0) = C_{24}(0) = c_0$, respectively] are discordant but not

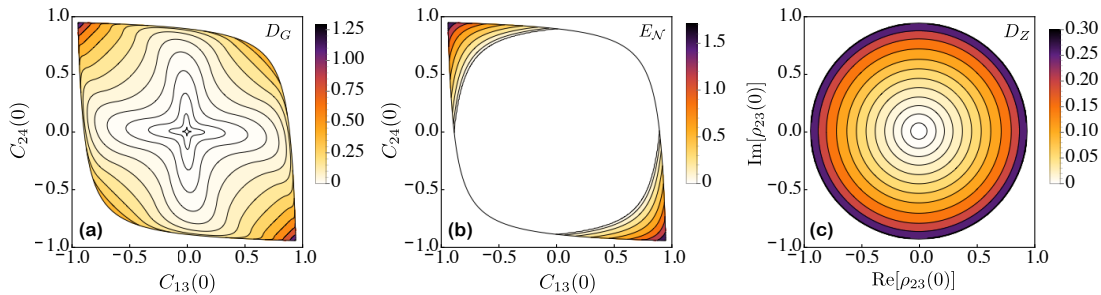


Figure 5. (Color online) Gaussian discord D_G (a) and logarithmic negativity E_N (b) of a state (31) as functions of $C_{13}(0)$ and $C_{24}(0)$ for $N_S=1$ and $N=0$. (c): Quantum discord D_Z of a state (41) as a function of $\text{Re}[\rho_{23}(0)]$ and $\text{Im}[\rho_{23}(0)]$ for $\xi_S=0.25$ and $\xi=1$. The states (41) considered for two qubits are never entangled.

entangled. For such states, Gaussian discord lies within a very narrow range (in general, the faster or slower the energy release the narrower the interval of possible values of D_G). Yet, based on figures 4 and 5, one can see that a high amount of discord does not necessarily lead to a fast or slow dissipation rate. Moreover, note that the most discordant state gives rise to the same heat flux time evolution as the completely uncorrelated state [see figure 4(c)]. The connection with energy release appears even weaker for entanglement as witnessed by the fact that, for each entangled state, there is always a separable one yielding the same heat flux dynamics [see figure 4(b)].

Overall, the above analysis indicates that it is the peculiar *structure* of correlations – instead of the featured amount of “quantumness” – that affects the heat flux dynamics. In particular, the quadratures that are most correlated plays the major role. The optimal situation indeed occurs when the pairs $\{\hat{X}_1, \hat{X}_2\}$ and $\{\hat{Y}_1, \hat{Y}_2\}$ are equally (anti)correlated by the highest possible amount.

VI. HEAT FLUX DYNAMICS: QUBITS

A. Thermal initial states

S now consists of a pair of qubits and both subsystems are initially in a local thermal state at temperature T_S , giving a joint (uncorrelated) initial state $\rho(0) = \exp[-\hat{H}_1/(k_B T_S)] \exp[-\hat{H}_2/(k_B T_S)]/Z_S^2$.

The corresponding density matrix has zero off-diagonal entries, while the diagonal ones read

$$\rho_{11}(0) = \frac{(1-\xi_S)^2}{4}, \quad \rho_{44}(0) = \frac{(1+\xi_S)^2}{4}, \quad (39)$$

$$\rho_{22}(0) = \rho_{33}(0) = \frac{1-\xi_S^2}{4}, \quad (40)$$

where ξ_S is the value taken by Eq. (9) for $T=T_S$.

One can use these (see Appendix C) to calculate the time evolution of the density matrix elements entering Eqs. (23)-(25), hence the heat fluxes $\mathcal{J}_1(t)$, $\mathcal{J}_2(t)$, $\mathcal{J}_{12}(t)$ and the total heat flux $J^{(c)}(t)$. Unfortunately, the resulting analytic expressions are rather involved and uninformative (even in limiting cases). It turns out that no general exact relations

as simple as those in Eqs. (27) and (28) can be established. Yet, many of the salient features of the heat flux dynamics are qualitatively quite similar to those emerging for harmonic oscillators. This is shown by the right-column plots of figure 2, where we plot \mathcal{J}_1 , \mathcal{J}_2 , \mathcal{J}_{12} and $J^{(c)}$ against time for different values of T/T_S (the same considered in Section V A). The shape of each curve is quite similar to the corresponding one in the case of harmonic oscillators [a minor difference is that at intermediate times $\mathcal{J}_2(t)$ and $J^{(c)}(t)$ are not as flat as those for continuous-variable systems]. As a distinctive feature, though, saturation appears at growing temperatures for each plotted quantity, which is clearly due to the fermionic nature of each subsystem as well as each reservoir mode.

B. Correlated initial states

In order to select a suitable family of correlated initial states $\rho(0)$, in full analogy with Subsection V B, we first require the local reduced qubit state to be locally thermal at temperature T_S . This entails that the only possible non-zero off-diagonal entries of $\rho(0)$ are $\rho_{23}(0) = \rho_{32}(0)^*$ and $\rho_{14}(0) = \rho_{41}(0)^*$ [the presence of extra off-diagonal entries would be incompatible with the constraint that each reduced state $\text{Tr}_i \rho(0)$ has a diagonal form]. In a way similar to Subsection V B, to simplify the analysis, we further restrict to states such that $\rho_{14}(0) = \rho_{41}(0) = 0$. Indeed, the heat fluxes in Eqs. (23)-(25) depend only on $\rho_{23}(t)$ and its c.c., which in turn are independent of $\rho_{14}(0)$ as shown in Appendix C.

Therefore,

$$\rho(0) = \frac{1}{4} \begin{pmatrix} (1-\xi_S)^2 & 0 & 0 & 0 \\ 0 & 1-\xi_S^2 & \rho_{23}(0) & 0 \\ 0 & \rho_{23}(0)^* & 1-\xi_S^2 & 0 \\ 0 & 0 & 0 & (1+\xi_S)^2 \end{pmatrix}. \quad (41)$$

The allowed values of $\rho_{23}(0)$ must fulfill the constraint

$$|\rho_{23}(0)| \leq 1-\xi_S^2 \quad (42)$$

which follows from the requirement that density matrix (41) be positive.

As in Subsection VB, we focus on the case of a zero-temperature reservoir (hence $\xi_N = 1$). From Eqs. (23)-(25) and initial state (41) – see also Appendix C – the heat fluxes are calculated as

$$\mathcal{J}_1(t) = \gamma(1 - \xi_S)e^{-\gamma t},$$

$$\mathcal{J}_2(t) = \gamma \left\{ (1 + \gamma^2 t^2) (1 - \xi_S) + 2(1 - \gamma t - e^{-\gamma t}) (1 - \xi_S)^2 - \gamma \text{Re}[\rho_{23}(0)] t \right\} e^{-\gamma t},$$

$$\mathcal{J}_{12}(t) = \gamma \left\{ 2(1 - e^{-\gamma t}) (1 - \xi_S)^2 - 2\gamma t(1 - \xi_S) + \text{Re}[\rho_{23}(0)] \right\} e^{-\gamma t}.$$

Note that heat fluxes depend on the initial correlations through $\text{Re}[\rho_{23}(0)]$. In figure 3(b), we use these results to plot the total heat flux, as given by Eq. (12), versus time for $\xi_S = 0.25$ and three representative values of $\text{Re}[\rho_{23}(0)]$.

As in the case of initial thermal states (see previous subsection), again we find a behaviour that qualitative resembles the one observed for harmonic oscillators (a minor difference occurs for the $\text{Re}[\rho_{23}(0)] = 0.75$ plot which does not feature stationary points but only concavity changes as time grows). This results from a comparison between figures 3(a) and 3(b), which shows that $\text{Re}[\rho_{23}(0)]$ here behaves similarly to the parameter $C_{13}(0) + C_{24}(0)$ for harmonic oscillators. Negative (positive) values of $\text{Re}[\rho_{23}(0)]$ cause a slow (fast) energy release.

In analogy with figure 4(a), in figure 6(a) we plot $\gamma\tau_p$ (time required to dissipate $p\%$ of the initial energy) for $\xi_S = 0$. The plots show that positive (negative) values of $\text{Re}[\rho_{23}(0)]$ always speed up (slow down) the energy release compared to the uncorrelated case. The relationship between the heat flux behaviour and the initial correlations can be better understood (see Appendix E) by expressing the superoperators (7, 8) and the initial state (41) in the collective basis $\{|ee\rangle, |\Psi^+\rangle, |\Psi^-\rangle, |gg\rangle\}$, where $|\Psi^\pm\rangle \equiv 1/\sqrt{2}(|eg\rangle_{12} \pm |ge\rangle_{12})$. Such rearrangement shows that states $|\Psi^+\rangle$ and $|\Psi^-\rangle$ are coupled to the environment with different strengths. In particular, the singlet $|\Psi^-\rangle$ is fully decoupled from the environment for $T = 0$. A positive initial value of ρ_{23} means a smaller initial population of $|\Psi^-\rangle$ and therefore a faster energy release. A negative initial value of $\text{Re}[\rho_{23}]$ means a larger initial population of $|\Psi^-\rangle$, hence a slower energy flow. This is shown in more detail in Appendix E

C. Influence of initial quantum correlations

In line with Subsection VC, we next investigate the connection between heat flux and typical measures of correlations of the initial state (41). These measures, namely the concurrence for entanglement and the quantum discord for general non-classical correlations, are described in Appendix F. Unlike family (31) for harmonic oscillators, all the qubit states (41) are *disentangled* (as can be shown by explicitly calculating the concurrence [35], see Appendix F). They all feature, however, some quantum discord D_Z . To show this, in figure 5(c) we set $\xi_S = 0.25$ and plot D_Z [36, 37] as a function of $\text{Re}[\rho_{23}(0)]$ and $\text{Im}[\rho_{23}(0)]$. Similarly to the behavior of D_G in figure 5(a), D_Z is non-zero on the entire plane but the origin $\text{Re}[\rho_{23}(0)] = \text{Im}[\rho_{23}(0)] = 0$.

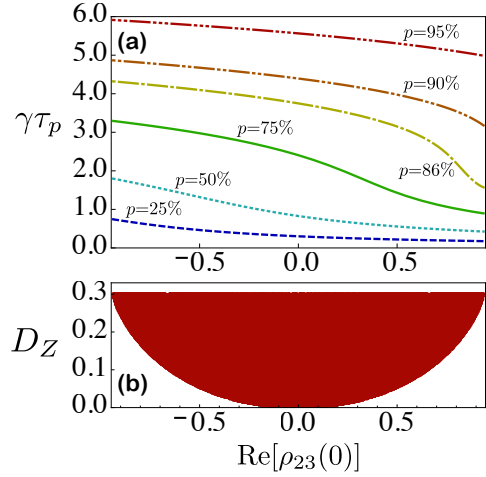


Figure 6. (Color online) (a): $\gamma\tau_p$ against $\text{Re}[\rho_{23}(0)]$ for $p = 95$ (red three-dotted-dashed line), $p = 90$ (orange two-dotted-dashed), $p = 86$ (yellow dot-dashed), $p = 75$ (green solid), $p = 50$ (cyan dotted) and $p = 25$ (blue dashed). (b): Quantum discord as a function of $\text{Re}[\rho_{23}(0)]$. Throughout, we have set $\xi_S = 0.25$ and $N = 0$.

In the present case, a simpler functional dependance arises since D_Z depends only on $|\rho_{23}(0)|$ and it is thus constant along each circle centred at the origin. As $|\rho_{23}(0)|$ grows up, D_Z increases.

We see that, similarly to harmonic oscillators, states with different discord can exhibit the same heat flux dynamics [corresponding to a set value of $\text{Re}[\rho_{23}(0)]$]. To better highlight this, in figure 6(b) for a fixed value of $\text{Re}[\rho_{23}(0)]$, we report all the possible values of D_Z . Similarly to the harmonic oscillators case, we see that the slowest and fastest heat flows occur only for the maximum value of discord. However, a high amount of discord does not necessarily imply a low or fast energy release as witnessed by the fact that states with maximum value of D_Z are compatible with any heat flux dynamics.

The above indicates that, also in the case of qubits, it is the structure of correlations that decides the speed of heat flux.

VII. INTERPRETATION OF CORRELATED HEAT FLUX FOR QUBITS

The non-local nature of the correlated heat \mathcal{J}_{12} [cf. Eqs. (12) and (14)] suggests a possible link between such quantity and some measure of correlations between S_1 and S_2 . A general formulation of such a connection with some known correlations indicator is not straightforward. Remarkably, however, we next find that, in the case of qubits, this is possible for a relevant class of initial states. Specifically, we show that \mathcal{J}_{12} can be expressed in terms of the so called *trace distance discord* (TDD) [38] whenever S is initially in a product of local thermal states. This is a well-behaved measure of non-classical correlations ex-

hibited by a bipartite quantum state (not necessarily in the presence of entanglement). Specifically, the one-sided trace distance discord (TDD) $\mathcal{D}_{\rightarrow}(\rho)$ from 1 to 2 of a bipartite quantum state ρ is defined as the minimal *trace norm* distance [25] between such state and the set of so called *classical-quantum* (CQ) states [38]. A CQ state features zero QCs with respect to local measurements on A and can be expressed as

$$\rho_{CQ} = \sum_j |\alpha_j\rangle_1 \langle \alpha_j| \otimes \varrho_2(j) \quad (43)$$

with $\{|\alpha_j\rangle_1\}$ being a complete set of orthonormal vectors of subsystem 1 and $\varrho_2(j)$ being a positive (not necessarily normalized) operator of subsystem 2. Specifically, if $\|\Theta\|_1 = \text{Tr}[\sqrt{\Theta^\dagger\Theta}]$ denotes the trace norm (or Schatten 1-norm) of a generic operator Θ then the TDD of state ρ is defined by

$$\mathcal{D}_{\rightarrow}(\rho) = \frac{1}{2} \min_{\{\rho_{CQ}\}} \|\rho - \rho_{CQ}\|_1, \quad (44)$$

where, as shown by the notation, the minimum is over all possible quantum-classical states (43). In other words, the TDD is the minimum distance in the Hilbert space between ρ and the set of CQ states.

We next restrict to a system S made out of a pair of qubits and initially in the state $\rho(0) = \frac{\exp[-\hat{H}_1/(k_B T_1)]}{Z_1} \otimes \frac{\exp[-\hat{H}_2/(k_B T_2)]}{Z_2}$, namely a tensor product of two local thermal states (in general at different temperatures). Note that such a family encompasses the initial state considered in Subsection VIA as a special case. Using the solution of the master equation given in Appendix C, it can be easily shown that the state of S will maintain the same form at any time (the local temperatures can change with time). A locally thermal state belongs to the family of two-qubit X states (these have non-zero entries on the two main diagonals of the corresponding density matrix). The TDD of such states can be calculated exactly [39]. Using the closed formula of Ref. [39], we find that at any time t the modulus of the correlated heat flux $\mathcal{J}_{12}(t)$ is proportional to the TDD of state $\rho(t)$ according to

$$|\mathcal{J}_{12}(t)| = 4\hbar\omega\gamma\xi \mathcal{D}_{\rightarrow}[\rho(t)]. \quad (45)$$

It is natural to wonder whether this property holds for more general initial states. This is not the case as can be seen through the following counterexample: let us select the initial state

$$\rho(0) = \frac{1}{2} |\psi\rangle_1 \langle \psi| \otimes \begin{pmatrix} 1 - \xi_2 & 0 \\ 0 & 1 + \xi_2 \end{pmatrix} \quad (46)$$

with

$$|\psi\rangle_1 = \sqrt{\frac{1+\xi}{2}} |0\rangle_1 + \sqrt{\frac{1-\xi}{2}} |1\rangle_1, \quad (47)$$

where ξ_2 is the same as in Eq. (9) for $T = T_2$. As in the previous case, $\rho(0)$ is a product state, hence featuring zero

correlations, with S_2 locally in a thermal state. Now, however, despite having the same populations and energy as the thermal state corresponding to ξ , the initial state of S_1 is fully *pure*. In other words, S_1 has the same temperature as R but features non-zero coherences. In such a case, we can show that $\mathcal{D}_{\rightarrow}(t)$ is in general finite but $\mathcal{J}_1(t) = \mathcal{J}_{12}(t) = 0$ identically. In other words, the interaction mediated by the reservoir gives rise to QCs between the system's subparts with no simultaneous development of any correlated heat flux.

VIII. CONCLUSIONS

In this work, we have studied the dynamics of heat flux of a bipartite system interacting with a thermal reservoir in a cascaded way. The cascading makes one of the two subsystems interact with the reservoir modified by the previous interaction with the other subsystem. Because of such circumstance, the local dynamics of the second subsystem is non-Markovian despite the fact that the joint dynamics is Markovian. This affects the heat flux in such a way that it exhibits a non-exponential time behaviour. We have carried out a systematic analysis of this after showing that the total heat flux can be decomposed into three components. In particular, one of these – arising from a non-local dissipator entering the master equation – can be identified as a correlated heat flux and was shown to play a major role in the non-monotonic time evolution.

Typical behaviours, occurring in the case of both thermal and correlated initial states, have been scrutinized for two paradigmatic systems: a pair of harmonic oscillators with a reservoir of bosonic modes and two qubits with a reservoir of fermionic modes. While in the case of harmonic oscillators basically all of the observed features can be explained analytically, an analogous analysis is not possible for qubits. Notwithstanding, most of the qualitative features of the heat flux dynamics are quite similar to those occurring for harmonic oscillators (aside from saturation effects owing to the presence of only two levels for qubits).

In the case of thermal initial states, we have shown that the total heat flux exhibits a monotonic, although non-exponential, time behaviour. In particular, an almost flat profile arises at intermediate times which is mostly due to the occurrence of the aforementioned correlated heat flux. To explore the effect of initial correlations in the system state, we have focused on a suitable family of initial states that are locally thermal but additionally feature non-local correlations. In general, the effect of these is to cause non-monotonicity of the total heat flux accompanied by a simultaneous slow down or speed up of the thermalisation process. We have investigated the role played by the initial amount of quantum correlations, either in the form of entanglement or discord, on the rate of energy exchange. Our analysis indicates that, although the states featuring the slowest and fastest heat flux dynamics are characterized by high values of discord, it is mostly the peculiar *structure* of initial correlations that matters rather than their overall amount.

Finally, we have found that – in the case of qubits and for initial thermal states – the magnitude of the correlated heat flux at any time coincides (up to a proportionality factor) with the trace distance discord of the open system. In particular, this shows the existence of a physical scenario within which such a *bona fide* measure of quantum correlations acquires a clear physical significance.

It is worth to emphasise that, as already observed, a key feature of our system is that while the joint dynamics of S_1 and S_2 is Markovian, the reduced dynamics of system S_2 is non-Markovian. Recently, the concept of quantum non-Markovianity has received remarkable attention [40] in the effort of defining on a rigorous basis the distinctive aspects of such phenomenon and, accordingly, ways to quantify it [41]. Within this framework, our work suggests an interesting connection between quantum non-Markovianity and

heat flux dynamics.

In this work, we have focused on initial states – either correlated or not – that are in any case locally thermal at a *uniform* temperature (i.e., the same for both subsystems). Allowing for a non-uniform temperature makes the heat flux dynamics as well as its interplay with initial correlations considerably richer, which will be the subject of a future work [42].

ACKNOWLEDGEMENTS

The authors are grateful to R. Fazio for useful discussions. This work is funded by the EU Collaborative Project TherMiQ (Grant Agreement 618074) and the Italian PRIN-MIUR 2010/2011.

-
- [1] J. Gemmer, M. Michel, and G. Mahler, *Quantum Thermodynamics: Emergence of Thermodynamic Behavior within Composite Quantum Systems*, Lect. Notes Phys. **657**, 2nd edition (Springer, Berlin, 2009).
- [2] J. Anders and V. Giovannetti New J. Phys. **15** 033022 (2013).
- [3] M. Horodecki and J. Oppenheim, Nat. Commun. **4**, 2059 (2013).
- [4] R. Alicki and M. Fannes, Phys. Rev. E **87**, 042123 (2013).
- [5] S. Mukamel, Phys. Rev. Lett. **90** 170604 (2003).
- [6] P. Talkner, E. Lutz and P. Hanggi, Phys. Rev. E **75** 050102 (2007).
- [7] M. Campisi, P. Talkner and P. Hanggi, Phys. Rev. Lett. **102** 210401 (2009).
- [8] M. Esposito, U. Harbola and S. Mukamel, Rev. Mod. Phys. **81** 1665 (2009).
- [9] M. Esposito, K. Lindenberg and C. Van den Broeck, New J. Phys. **12** 013013 (2010).
- [10] M. Campisi, P. Hanggi and P. Talkner, Rev. Mod. Phys. **83** 771 (2011).
- [11] R. Alicki, J. Phys. A **12**, L103 (1979).
- [12] G. Lindblad, Comm. Math. Phys. **48**, 119 (1976).
- [13] M. B. Plenio and S. Virmani, Phys. Rev. Lett. **99**, 120504 (2007).
- [14] F. Caruso, V. Giovannetti, and G. M. Palma, Phys. Rev. Lett. **104**, 020503 (2010).
- [15] G. Benenti, A. D’Arrigo, and G. Falci, Phys. Rev. Lett. **103**, 020502 (2009).
- [16] F. Caruso, V. Giovannetti, C. Lupo, and S. Mancini, Rev. Mod. Phys. **86**, 59 (2012).
- [17] R. Horodecki, P. Horodecki, M. Horodecki, and K. Horodecki, Rev. Mod. Phys. **81**, 865 (2009).
- [18] K. Modi, A. Brodutch, H. Cable, T. Paterek, and V. Vedral, Rev. Mod. Phys. **84**, 1655 (2012).
- [19] M. Mohseni, P. Rebentrost, S. Lloyd, and A. Aspuru-Guzik, Journal of Chemical Physics **129**, 174106 (2008).
- [20] M. B. Plenio and S. F. Huelga, New J. Phys. **10**, 113019 (2008).
- [21] P. Lambropoulos and D. Petrosyan, *Fundamentals of Quantum Optics and Quantum Information* (Cambridge University Press, Cambridge, U. K., 2007).
- [22] C. W. Gardiner and M. J. Collett, Phys. Rev. A **31**, 3761 (1985).
- [23] C. W. Gardiner and A. S. Parkins, Phys. Rev. A **50**, 1792 (1994).
- [24] V. Giovannetti and G. M. Palma, Phys. Rev. Lett. **108**, 040401 (2012).
- [25] M. A. Nielsen and I. L. Chuang, *Quantum Computation and Quantum Information* (Cambridge University Press, Cambridge, U. K., 2000).
- [26] C. W. Gardiner, Phys. Rev. Lett. **70**, 2269 (1993).
- [27] H. Breuer and F. Petruccione, *The Theory of Open Quantum Systems* (Oxford University Press, Oxford, 2002).
- [28] C. W. Gardiner and P. Zoller, *Quantum Noise* (Springer, Berlin, 2000).
- [29] A. Ferraro, S. Olivares, and M. G. A. Paris, *Gaussian states in continuous variable quantum information* (Bibliopolis, Napoli, 2005).
- [30] K. Stannigel, P. Rabl, and P. Zoller, New J. Phys. **14**, 063014 (2012).
- [31] G. Vidal and R. F. Werner, Phys. Rev. A **65**, 032314 (2002).
- [32] G. Adesso and A. Datta, Phys. Rev. Lett. **105**, 030501 (2010).
- [33] The former point is such that the variances $\langle(\hat{X}_1 - \hat{X}_2)^2\rangle = 2[C_{11}(0) - C_{13}(0)]$ and $\langle(\hat{Y}_1 + \hat{Y}_2)^2\rangle = 2[C_{11}(0) + C_{24}(0)]$ are both zero, while for the latter one the variances $\langle(\hat{X}_1 + \hat{X}_2)^2\rangle = 2[C_{11}(0) + C_{13}(0)]$ and $\langle(\hat{Y}_1 - \hat{Y}_2)^2\rangle = 2[C_{11}(0) - C_{24}(0)]$ simultaneously vanish.
- [34] A. Einstein, B. Podolsky, and N. Rosen, Phys. Rev. **47**, 777 (1935).
- [35] W. K. Wootters, Phys. Rev. Lett. **80**, 2245 (1998).
- [36] H. Ollivier and W. H. Zurek, Phys. Rev. Lett. **88**, 017901 (2001).
- [37] B. Dakic, V. Vedral, and C. Brukner, Phys. Rev. Lett. **105**, 190502 (2010).
- [38] T. Debarba, T. O. Maciel, and R. O. Vianna, Phys. Rev. A **86**, 024302 (2012); S. Rana and P. Parashar, Phys. Rev. A **87**, 016301 (2013); T. Nakano, M. Piani, and G. Adesso, Phys. Rev. A **88**, 012117 (2013).
- [39] F. Ciccarello, T. Tufarelli, and V. Giovannetti, New J. Phys. **16**, 013038 (2014).
- [40] A. Rivas and S.F. Huelga, *Open Quantum Systems. An Introduction* (Springer, Heidelberg, 2011); H.-P. Breuer, J. Phys. B: At. Mol. Opt. Phys. **45**, 154001 (2012); A. Rivas, S. F. Huelga, and M. B. Plenio, Rep. Prog. Phys. **77**,

- 094001 (2014).
- [41] H.-P. Breuer, E.-M. Laine, and J. Piilo, Phys. Rev. Lett. **103**, 210401 (2009); A. Rivas, S. F. Huelga, M. B. Plenio, Phys. Rev. Lett. **105**, 050403 (2010); S. Luo, S. Fu, and H. Song, Phys. Rev. A **86**, 044101 (2012); S. Lorenzo, F. Plastina, and M. Paternostro, Phys. Rev. A **88**, 020102(R) (2013); D. Chruściński and S. Maniscalco, Phys. Rev. Lett. **112**, 120404 (2014).
- [42] A. Farace *et al.*, in preparation.
- [43] S. Mukamel, *Principles of Nonlinear Optical Spectroscopy* (Oxford University Press, New York, 1995).
- [44] S. Pirandola, A. Serafini, and S. Lloyd, Phys. Rev. A **79**, 052327 (2009).
- [45] B. Groisman, S. Popescu, and A. Winter, Phys. Rev. A **72**, 032317 (2005).
- [46] P. Giorda and M. G. A. Paris, Phys. Rev. Lett. **105**, 020503 (2010).
- [47] P. Giorda, M. Allegra and M. G. A. Paris, Phys. Rev. A **86**, 052328 (2012).
- [48] S. Olivares and M. G. A. Paris, Int. J. Mod. Phys. B **27**, 1345024 (2013).
- [49] A. Peres, Phys. Rev. Lett. **77**, 1413 (1996).
- [50] R. Simon, Phys. Rev. Lett. **84**, 2726 (2000).

Appendix A: Stationary state

Here, we prove that the thermal state (10) is indeed the asymptotic state reached by S both in the case of har-

$$\begin{aligned}
\mathcal{L}_1(\rho_{\text{th}}) &= \left[\gamma(N+1) \left(e^{-\beta\hbar\omega\hat{a}_1^\dagger\hat{a}_1} e^{-\beta\hbar\omega\hat{a}_1\hat{a}_1^\dagger} - e^{-\beta\hbar\omega\hat{a}_1^\dagger\hat{a}_1} \hat{a}_1^\dagger\hat{a}_1 \right) + \gamma N \left(e^{-\beta\hbar\omega\hat{a}_1^\dagger\hat{a}_1} e^{\beta\hbar\omega\hat{a}_1^\dagger\hat{a}_1} - e^{-\beta\hbar\omega\hat{a}_1^\dagger\hat{a}_1} \hat{a}_1^\dagger\hat{a}_1 - e^{-\beta\hbar\omega\hat{a}_1^\dagger\hat{a}_1} \right) \right] e^{-\beta\hbar\omega\hat{a}_2^\dagger\hat{a}_2} \\
&= \left[\gamma(N+1)(e^{-\beta\hbar\omega} - 1)\hat{a}_1^\dagger\hat{a}_1 + \gamma(N+1)e^{-\beta\hbar\omega} + \gamma N(e^{\beta\hbar\omega} - 1)\hat{a}_1^\dagger\hat{a}_1 - \gamma N \right] \rho_{\text{th}} \\
&= (-\gamma\hat{a}_1^\dagger\hat{a}_1 + \gamma N + \gamma\hat{a}_1^\dagger\hat{a}_1 - \gamma N)\rho_{\text{th}} = 0.
\end{aligned}$$

monic oscillators and qubits. Let $\rho_{\text{th}} = e^{-\beta\hat{H}_1} e^{-\beta\hat{H}_2}$ with $\beta = 1/(k_B T)$ (the tensor product symbol is omitted for simplicity). To demonstrate that this is indeed the system's steady state, we will prove that ρ_{th} fulfils the master equation under stationary conditions (when all the time derivatives vanish), namely

$$(\mathcal{L}_1 + \mathcal{L}_2 + \mathcal{D}_{12})(\rho_{\text{th}}) = 0. \quad (\text{A1})$$

a. Harmonic oscillators

Let $\hat{U}_\pm = e^{\pm\beta\hbar\omega\hat{a}^\dagger\hat{a}}$, where \hat{a} and \hat{a}^\dagger are bosonic annihilation and creation operators. Then, $\hat{U}_-\hat{a}\hat{U}_+ = e^{\beta\hbar\omega}\hat{a}$ and $\hat{U}_-\hat{a}^\dagger\hat{U}_+ = e^{-\beta\hbar\omega}\hat{a}^\dagger$. These identities entail

$$\left[e^{-\beta\hbar\omega\hat{a}^\dagger\hat{a}}, \hat{a} \right] = (1 - e^{-\beta\hbar\omega}) e^{-\beta\hbar\omega\hat{a}^\dagger\hat{a}} \hat{a}, \quad (\text{A2})$$

$$\left[e^{-\beta\hbar\omega\hat{a}^\dagger\hat{a}}, \hat{a}^\dagger \right] = (1 - e^{\beta\hbar\omega}) e^{-\beta\hbar\omega\hat{a}^\dagger\hat{a}} \hat{a}^\dagger. \quad (\text{A3})$$

In the present case, $\rho_{\text{th}} = e^{-\beta\hbar\omega\hat{a}_1^\dagger\hat{a}_1} e^{-\beta\hbar\omega\hat{a}_2^\dagger\hat{a}_2}$. Applying \mathcal{L}_1 [cf. Eq. (4)] to such a state, upon use of Eqs. (A2) and (A3), yields

Likewise, the identity $\mathcal{L}_2(\rho_{\text{th}}) = 0$ is proven by swapping indexes 1 and 2. The last step is thus showing that $\mathcal{D}_{12}\rho_{\text{th}} = 0$ (cf. Eq. (5)). Using again eqs (A2) and (A3) gives

$$\begin{aligned}
\mathcal{D}_{12}(\rho_{\text{th}}) &= \left\{ \gamma(N+1) \left[e^{-\beta\hbar\omega} (1 - e^{\beta\hbar\omega}) \hat{a}_1\hat{a}_2^\dagger - (1 - e^{-\beta\hbar\omega}) \hat{a}_1^\dagger\hat{a}_2 \right] + \gamma N \left[e^{\beta\hbar\omega} (1 - e^{-\beta\hbar\omega}) \hat{a}_1^\dagger\hat{a}_2 - (1 - e^{\beta\hbar\omega}) \hat{a}_1\hat{a}_2^\dagger \right] \right\} \rho_{\text{th}} \\
&= \left[\gamma(N+1)e^{-\beta\hbar\omega} (1 - e^{\beta\hbar\omega}) \hat{a}_1\hat{a}_2^\dagger - \gamma N (1 - e^{\beta\hbar\omega}) \hat{a}_1\hat{a}_2^\dagger - \gamma(N+1)(1 - e^{-\beta\hbar\omega}) \hat{a}_1^\dagger\hat{a}_2 + \gamma N e^{\beta\hbar\omega} (1 - e^{-\beta\hbar\omega}) \hat{a}_1^\dagger\hat{a}_2 \right] \rho_{\text{th}} \\
&= \left[\gamma N (1 - e^{\beta\hbar\omega}) \hat{a}_1\hat{a}_2^\dagger - \gamma N (1 - e^{\beta\hbar\omega}) \hat{a}_1\hat{a}_2^\dagger - \gamma(N+1)(1 - e^{-\beta\hbar\omega}) \hat{a}_1^\dagger\hat{a}_2 + \gamma(N+1)(1 - e^{-\beta\hbar\omega}) \hat{a}_1^\dagger\hat{a}_2 \right] \rho_{\text{th}} = 0.
\end{aligned}$$

This concludes the proof.

b. Qubits

In this case $\rho_{\text{th}} = e^{-\beta\hat{H}_1} e^{-\beta\hat{H}_2} / Z^2$, which we rearrange as $\rho_{\text{th}} = \rho_{1\text{th}}\rho_{2\text{th}}$ with

$$\rho_{i\text{th}} = \frac{1}{Z} \left(\frac{\mathbb{1}_i}{2} - \frac{\xi}{2} \hat{\sigma}_{iz} \right). \quad (\text{A4})$$

Using $\hat{\sigma}_{j\pm}\hat{\sigma}_{jz}\sigma_{j\mp} = \mp\sigma_{j\pm}\hat{\sigma}_{j\mp}$ and $\hat{\sigma}_{jz}\hat{\sigma}_{j\pm}\hat{\sigma}_{j\mp} = \hat{\sigma}_{j\pm}\hat{\sigma}_{j\mp}\sigma_{jz} = \pm\hat{\sigma}_{j\pm}\hat{\sigma}_{j\mp}$ it is immediate to see that $\mathcal{L}_i(\rho_{\text{th}}) = 0$ [cf. (7)] since $\mathcal{L}_i(\mathbb{1}_i) = \xi\mathcal{L}_i(\hat{\sigma}_{iz})$.

On the other hand, from Eq. (8) follows

$$\begin{aligned} \mathcal{D}_{12}(\rho_{\text{th}}) = & \hat{\sigma}_{1-} \frac{\gamma}{2} [\hat{\sigma}_{1-}, \rho_1^{\text{th}}] [\rho_2^{\text{th}}, \hat{\sigma}_{2+}] + \frac{\gamma}{2} [\hat{\sigma}_{1+}, \rho_1^{\text{th}}] [\rho_2^{\text{th}}, \hat{\sigma}_{2-}] \\ & + \frac{\gamma\xi}{2} \{\hat{\sigma}_{1-}, \rho_1^{\text{th}}\} [\rho_2^{\text{th}}, \hat{\sigma}_{2+}] - \frac{\gamma\xi}{2} \{\hat{\sigma}_{1+}, \rho_1^{\text{th}}\} [\rho_2^{\text{th}}, \hat{\sigma}_{2-}], \end{aligned}$$

which upon use of $[\hat{\sigma}_k^\pm, \rho_k^{\text{th}}] = \pm\xi\hat{\sigma}_k^\pm$ and $\{\hat{\sigma}_k^\pm, \rho_k^{\text{th}}\} = \hat{\sigma}_k^\pm$ yields

$$\begin{aligned} \mathcal{D}^{12}[\rho_{\text{th}}] = & \frac{\gamma\xi}{2} (-\hat{\sigma}_1^-) (-\xi\hat{\sigma}_2^+) + \frac{\gamma\xi}{2} (\hat{\sigma}_1^+) (\xi\hat{\sigma}_2^-) \\ & + \frac{\gamma\xi}{2} (\hat{\sigma}_1^-) (-\xi\hat{\sigma}_2^+) - \frac{\gamma\xi}{2} (\hat{\sigma}_1^+) (\xi\hat{\sigma}_2^-) = 0. \end{aligned} \quad (\text{A5})$$

This concludes the proof.

Appendix B: Time evolution of the covariance matrix for harmonic oscillators

For a given initial state, the explicit calculation of the coefficients $C_{mn}(t)$ entering the heat fluxes in Eqs. (20)-(22) is conveniently carried out through the Langevin equations [23]. These are equivalent to the master equation (1) and read

$$\frac{d}{dt} \begin{pmatrix} \hat{X}_1 \\ \hat{Y}_1 \\ \hat{X}_2 \\ \hat{Y}_2 \end{pmatrix} = -\gamma \begin{pmatrix} \frac{1}{2} & 0 & 0 & 0 \\ 0 & \frac{1}{2} & 0 & 0 \\ 1 & 0 & \frac{1}{2} & 0 \\ 0 & 1 & 0 & \frac{1}{2} \end{pmatrix} \begin{pmatrix} \hat{X}_1 \\ \hat{Y}_1 \\ \hat{X}_2 \\ \hat{Y}_2 \end{pmatrix} - \sqrt{\gamma} \begin{pmatrix} \hat{X}_{\text{in}} \\ \hat{Y}_{\text{in}} \\ \hat{X}_{\text{in}} \\ \hat{Y}_{\text{in}} \end{pmatrix}, \quad (\text{B1})$$

where \hat{X}_{in} and \hat{Y}_{in} are zero-mean Gaussian noises characterized by the correlations $\langle \hat{X}_{\text{in}} \hat{Y}_{\text{in}} \rangle = 0$, $\langle \hat{X}_{\text{in}} \hat{X}_{\text{in}} \rangle = \langle \hat{Y}_{\text{in}} \hat{Y}_{\text{in}} \rangle = N + \frac{1}{2}$. Correspondingly, the covariance matrix evolves in time as

$$\frac{d}{dt} C = AC + CA^T + M, \quad (\text{B2})$$

where A is the matrix appearing in Eq. (B1) and

$$M = \gamma \left(N + \frac{1}{2} \right) \begin{pmatrix} 1 & 0 & 1 & 0 \\ 0 & 1 & 0 & 1 \\ 1 & 0 & 1 & 0 \\ 0 & 1 & 0 & 1 \end{pmatrix}. \quad (\text{B3})$$

The solution of such a linear first-order differential system yields the covariance matrix vs. time and, in particular, the time-dependent coefficients appearing in Eqs. (20)-(22). The relevant equations are

$$\dot{C}_{11}(t) = -\gamma [C_{11}(t) - (N + \frac{1}{2})], \quad (\text{B4})$$

$$\dot{C}_{22}(t) = -\gamma [C_{22}(t) - (N + \frac{1}{2})], \quad (\text{B5})$$

$$\dot{C}_{33}(t) = -\gamma [C_{33}(t) - (N + \frac{1}{2})] - 2\gamma C_{13}(t), \quad (\text{B6})$$

$$\dot{C}_{44}(t) = -\gamma [C_{44}(t) - (N + \frac{1}{2})] - 2\gamma C_{24}(t), \quad (\text{B7})$$

$$\dot{C}_{13}(t) = -\gamma C_{13}(t) - \gamma [C_{11}(t) - (N + \frac{1}{2})], \quad (\text{B8})$$

$$\dot{C}_{24}(t) = -\gamma C_{24}(t) - \gamma [C_{22}(t) - (N + \frac{1}{2})], \quad (\text{B9})$$

$$\dot{C}_{12}(t) = -\gamma C_{12}(t), \quad (\text{B10})$$

$$\dot{C}_{14}(t) = -\gamma C_{14}(t) - \gamma C_{12}(t), \quad (\text{B11})$$

$$\dot{C}_{23}(t) = -\gamma C_{23}(t) - \gamma C_{12}(t), \quad (\text{B12})$$

$$\dot{C}_{34}(t) = -\gamma C_{34}(t) - \gamma C_{14}(t) - \gamma C_{23}(t). \quad (\text{B13})$$

We thus find two independent families of equations: one for the $\langle X_i X_j \rangle$, $\langle Y_i Y_j \rangle$ correlations and one for $\langle X_i Y_j \rangle$. In particular, Eqs. (B4)-(B9) completely determine the evolution of the heat flux as can be seen upon inspection of Eqs. (20)-(22).

Appendix C: Time evolution of the density matrix for qubits

In the Liouville space [43], the density operator of the two qubits S_1 and S_2 reads

$$\rho(t) = \sum_{kj} \text{Tr}[\rho(t)|j\rangle\langle k||k\rangle\langle j|] = \sum_{kj} \rho_{kj}(t) |kj\rangle \quad (\text{C1})$$

with $k, j = 1, \dots, 4$, $|1\rangle \equiv |ee\rangle_{12}$, $|2\rangle \equiv |eg\rangle_{12}$, $|3\rangle \equiv |ge\rangle_{12}$ and $|4\rangle \equiv |gg\rangle_{12}$ and where we have adopted a double-bracket notation according to which $|kj\rangle \equiv |k\rangle|j\rangle$ is a vector in the Liouville space vector. Hence, in such a space ρ is a vector expressed as a linear combination of the basis vectors $\{|kj\rangle\}$ (vectorization). Accordingly, master equation (1) can be written in the matrix form $\dot{\rho} = \mathcal{K}\rho$, where matrix \mathcal{K} is defined by $\mathcal{K}_{kj,mn} = \langle\langle kj | \mathcal{L} | mn \rangle\rangle = \text{Tr}\{|j\rangle\langle k | \mathcal{L}(|m\rangle\langle n|)\}$. In our case, such matrix is explicitly given by

$$\frac{\mathcal{K}}{2\gamma} = \begin{pmatrix} -2(1+\xi) & 0 & 0 & 0 & 0 & 1-\xi & 1-\xi & 0 & 0 & 1-\xi & 1-\xi & 0 & 0 & 0 & 0 & 0 \\ 0 & -2-\xi & \xi-1 & 0 & 0 & 0 & 0 & 1-\xi & 0 & 0 & 0 & 1-\xi & 0 & 0 & 0 & 0 \\ 0 & -1-\xi & -2-\xi & 0 & 0 & 0 & 0 & 1-\xi & 0 & 0 & 0 & 1-\xi & 0 & 0 & 0 & 0 \\ 0 & 0 & 0 & -2 & 0 & 0 & 0 & 0 & 0 & 0 & 0 & 0 & 0 & 0 & 0 & 0 \\ 0 & 0 & 0 & 0 & -2-\xi & 0 & 0 & 0 & \xi-1 & 0 & 0 & 0 & 0 & 1-\xi & 1-\xi & 0 \\ 1+\xi & 0 & 0 & 0 & 0 & -2 & \xi-1 & 0 & 0 & \xi-1 & 0 & 0 & 0 & 0 & 0 & 1-\xi \\ 1+\xi & 0 & 0 & 0 & 0 & -1-\xi & -2 & 0 & 0 & \xi-1 & 0 & 0 & 0 & 0 & 0 & 1-\xi \\ 0 & 1+\xi & 1+\xi & 0 & 0 & 0 & 0 & -2+\xi & 0 & 0 & 0 & \xi-1 & 0 & 0 & 0 & 0 \\ 0 & 0 & 0 & 0 & -1-\xi & 0 & 0 & 0 & -2-\xi & 0 & 0 & 0 & 0 & 1-\xi & 1-\xi & 0 \\ 1+\xi & 0 & 0 & 0 & 0 & -1-\xi & 0 & 0 & -2 & \xi-1 & 0 & 0 & 0 & 0 & 0 & 1-\xi \\ 1+\xi & 0 & 0 & 0 & 0 & -1-\xi & 0 & 0 & -1-\xi & -2 & 0 & 0 & 0 & 0 & 0 & 1-\xi \\ 0 & 1+\xi & 1+\xi & 0 & 0 & 0 & 0 & -1-\xi & 0 & 0 & 0 & -2+\xi & 0 & 0 & 0 & 0 \\ 0 & 0 & 0 & 0 & 0 & 0 & 0 & 0 & 0 & 0 & 0 & 0 & -2 & 0 & 0 & 0 \\ 0 & 0 & 0 & 0 & 1+\xi & 0 & 0 & 0 & 1+\xi & 0 & 0 & 0 & 0 & -2+\xi & \xi-1 & 0 \\ 0 & 0 & 0 & 0 & 1+\xi & 0 & 0 & 0 & 1+\xi & 0 & 0 & 0 & 0 & -1-\xi & -2+\xi & 0 \\ 0 & 0 & 0 & 0 & 0 & 1+\xi & 1+\xi & 0 & 0 & 1+\xi & 1+\xi & 0 & 0 & 0 & 0 & 2(\xi-1) \end{pmatrix},$$

where we have used the ordering

$$\begin{pmatrix} \mathcal{K}_{11,11} & \mathcal{K}_{11,12} & \mathcal{K}_{11,13} & \mathcal{K}_{11,14} & \mathcal{K}_{11,21} & \cdots \\ \mathcal{K}_{21,11} & \mathcal{K}_{21,12} & \mathcal{K}_{21,13} & \mathcal{K}_{21,14} & \mathcal{K}_{21,21} & \\ \mathcal{K}_{31,11} & \mathcal{K}_{31,12} & \mathcal{K}_{31,13} & \mathcal{K}_{31,14} & \mathcal{K}_{31,21} & \\ \mathcal{K}_{41,11} & \mathcal{K}_{41,12} & \mathcal{K}_{41,13} & \mathcal{K}_{41,14} & \mathcal{K}_{41,21} & \\ \mathcal{K}_{12,11} & \mathcal{K}_{12,12} & \mathcal{K}_{12,13} & \mathcal{K}_{12,14} & \mathcal{K}_{12,21} & \\ \vdots & & & & & \ddots \end{pmatrix}. \quad (\text{C2})$$

The solution of the linear first-order differential system $\dot{\rho} = \mathcal{K}\rho$ is found in an exponential form as

$$\rho_{mn}(t) = \sum_{k,j} (e^{\mathcal{K}t})_{mn,kj} \rho_{kj}(0). \quad (\text{C3})$$

In particular, it turns out that

$$\rho_{14}(t) = e^{-\gamma t} \rho_{14}(0), \quad (\text{C4})$$

which shows that the off-diagonal terms $\rho_{14}(t) = \rho_{41}(t)^*$ are decoupled from other elements of the density matrix regardless of the system initial state.

Appendix D: Parametrization of initial correlated states for harmonic oscillators

As discussed in the main text (Section VI), in the case of harmonic oscillators we focus on the family of initial states whose associated covariance matrix reads

$$C(0) = \begin{pmatrix} C_{11}(0) & 0 & C_{13}(0) & 0 \\ 0 & C_{11}(0) & 0 & C_{24}(0) \\ C_{13}(0) & 0 & C_{11}(0) & 0 \\ 0 & C_{24}(0) & 0 & C_{11}(0) \end{pmatrix}, \quad (\text{D1})$$

where $C_{11}(0) = N_S + \frac{1}{2}$ and the total energy is fixed to $U = \frac{1}{2}\text{Tr}[C(0)] = 2C_{11}(0)$. This choice is motivated by the fact that the heat flux depends only on $C_{ii}(t)$, $C_{13}(t)$, $C_{24}(t)$ (see Eqs. (20)-(22)) and these instantaneous values are completely determined by the initial conditions $C_{ii}(0)$, $C_{13}(0)$, $C_{24}(0)$ (see Eqs. (B4)-(B9)). We could then choose any value for the remaining off-diagonal terms without affecting the heat flux, but the optimal choice is zero, as argued at the end of the section. Our essential task is to derive the conditions on the off-diagonal elements $C_{13}(0)$ and

$C_{24}(0)$, in order for $C(0)$ to describe a physical state once the total energy is fixed. In general, a covariance matrix of a physically admissible Gaussian state must be such that all the second moments fulfill the Heisenberg uncertainty relations. This requirement can be expressed compactly as the semi-positivity condition

$$C(0) + \frac{i}{2} \begin{pmatrix} 0 & 1 & 0 & 0 \\ -1 & 0 & 0 & 0 \\ 0 & 0 & 0 & 1 \\ 0 & 0 & -1 & 0 \end{pmatrix} \geq 0. \quad (\text{D2})$$

This is equivalent to two necessary and sufficient conditions [44]. First, the covariance matrix needs to be positive, i.e., $C(0) > 0$, which is in turn equivalent to the two inequalities

$$|C_{13}(0)| < C_{11}(0) = N_S + \frac{1}{2}, \quad |C_{24}(0)| < N_S + \frac{1}{2}. \quad (\text{D3})$$

Second, the symplectic eigenvalues ν_{\pm} must fulfil

$$\nu_{\pm} = \sqrt{\frac{I_A + I_B + 2I_C \pm \sqrt{(I_A + I_B + 2I_C)^2 - 4I_{\Sigma}}}{2}} \geq \frac{1}{2}, \quad (\text{D4})$$

where we introduced the symplectic invariants [29] $I_A = I_B = C_{11}(0)^2$, $I_C = C_{13}(0)C_{24}(0)$ and $I_{\Sigma} = C_{11}(0)^4 + C_{13}(0)^2 C_{24}(0)^2 - C_{11}(0)^2 [C_{13}(0)^2 + C_{24}(0)^2]$. Note that if the pair $\{C_{13}(0), C_{24}(0)\} = \{c, d\}$ satisfies the two conditions, so do the pairs $\{C_{13}(0), C_{24}(0)\} = \{d, c\}$ and $\{C_{13}(0), C_{24}(0)\} = \{-c, -d\}$. Hence, the region of physicality is symmetric across the two diagonals of the $C_{13}(0) - C_{24}(0)$ plane. In figure 7, we plot this region for different values of N_S . One can see that the area of the physicality region grows with N_S . Indeed, if $N_S = 0$ each local state [i.e., $\rho_1(0)$ and $\rho_2(0)$] is pure since S is in the vacuum state, hence no correlations are present. Moreover, note that the line where $C_{13}(0) = C_{24}(0)$ (red line in figure ...) spans all the allowed values of $C_{13}(0) + C_{24}(0)$ (this is constant along each black dashed line in the plots). As heat fluxes depend on $C_{13}(0)$ and $C_{24}(0)$ through their sum $C_{13}(0) + C_{24}(0)$ [cf. Eqs. (32)-(34)], we see that, in order to explore all the possible heat flux dynamics, one can set $C_{13}(0) = C_{24}(0)$ without loss of generality. In other words, given a black dashed line (see figure 7), any covariance matrix lying on it yields the same heat flux dynamics as that associated with its intersection point with the red line. Moreover, for states such that $C_{13}(0) = C_{24}(0)$ the constraints (D3) and (D4) can be combined into the single condition $|C_{13}(0)| \leq N_S$.

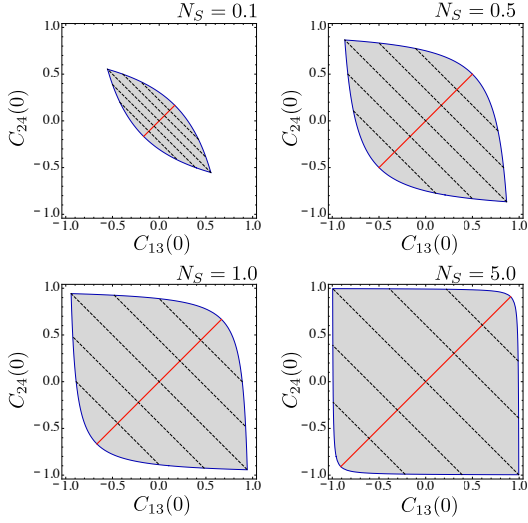


Figure 7. (Color online) Domain on the $C_{13}(0) - C_{24}(0)$ plane within which the covariance matrix represents a physical Gaussian state for different values of N_S , i.e., the total energy. Both $C_{13}(0)$ and $C_{24}(0)$ are expressed in units of $N_S + 1/2$. The sum $C_{13}(0) + C_{24}(0)$ is constant along each black dashed line. The red dashed line is instead the set of points such that $C_{13}(0) = C_{24}(0)$.

This entails that, in the light of the above considerations,

$$|C_{13}(0) + C_{24}(0)| \leq 2N_S. \quad (\text{D5})$$

If we had other non-zero off-diagonal terms, the constraints (D3) and (D4) would be more restrictive on $C_{13}(0)$ and $C_{24}(0)$. In other words we would get $|C_{13}(0) + C_{24}(0)| \leq C_{MAX} < 2N_S$ and some possible evolutions of the heat flux would remain unexplored. Starting with a state of the form (D1) allows instead for a complete analysis of the problem.

Appendix E: Role of initial correlations

Introducing the collective basis $\{|ee\rangle, |\Psi^+\rangle, |\Psi^-\rangle, |gg\rangle\}$, where $|\Psi^\pm\rangle \equiv 1/\sqrt{2}(|eg\rangle_{12} \pm |ge\rangle_{12})$, the initial state (41) becomes

$$\rho(0) = \frac{1}{4} \begin{pmatrix} (1-\xi_S)^2 & 0 & 0 & 0 \\ 0 & 1-\xi_S^2 + \text{Re}[\rho_{23}(0)] & 0 & 0 \\ 0 & 0 & 1-\xi_S^2 - \text{Re}[\rho_{23}(0)] & 0 \\ 0 & 0 & 0 & (1+\xi_S)^2 \end{pmatrix}. \quad (\text{E1})$$

Clearly, a positive (negative) value of $\text{Re}[\rho_{23}]$ means a smaller (larger) initial population of $|\Psi^-\rangle$ compared to the case where $\text{Re}[\rho_{23}] = 0$. On other hand, master equation (1) can be reexpressed as [30]

$$\dot{\rho} = -i [\tilde{H}, \rho] + \tilde{\mathcal{L}}(\rho), \quad (\text{E2})$$

where we have defined

$$\tilde{\mathcal{L}}(\rho) = \Gamma^+ \mathcal{L}[|\Psi^+\rangle\langle gg| + |ee\rangle\langle\Psi^+|](\rho) + \Gamma^- \mathcal{L}[|\Psi^-\rangle\langle gg| - |ee\rangle\langle\Psi^-|](\rho), \quad (\text{E3})$$

$$\tilde{H} = H - i\frac{\gamma}{2} (|\Psi^+\rangle\langle\Psi^-| - |\Psi^-\rangle\langle\Psi^+|) \quad (\text{E4})$$

with $\mathcal{L}[\hat{o}](\rho) = \hat{o}\rho\hat{o}^\dagger - \frac{1}{2}\{\hat{o}\hat{o}^\dagger, \rho\}$ for a generic operator \hat{o} and $\Gamma^\pm = (1 \pm \xi)/2$. It is clear that for $N=0$, i.e., $\xi=1$, as in the plot in fig. 6, $|\Psi^-\rangle$ is not directly affected by dissipation, which yields a slow down of energy releasing if $\text{Re}[\rho_{23}] < 0$.

Appendix F: Computation of quantum correlations

1. Discord-like measures

Given a pair of quantum systems A and B , quantum discord [36] is the gap between two classically equivalent expressions of the mutual information content given by

$$\mathcal{D}(B|A) = \mathcal{I}(AB) - \mathcal{C}(B|A), \quad (\text{F1})$$

where

$$\mathcal{I}(AB) = S(\rho_A) + S(\rho_B) - S(\rho_{AB}), \quad (\text{F2})$$

is quantum mutual information [45], while

$$\mathcal{C}(B|A) = \max_{\{E_a\}} \left[S(\rho_B) - \sum_a p_a S\left(\frac{\text{Tr}_A[\rho_{AB} E_a]}{p_a}\right) \right]. \quad (\text{F3})$$

is interpreted as the total amount of classical correlations in the above expression. Here, $S(\rho)$ is the Von Neumann entropy, $\sum_a E_a = \mathbb{1}$ is a positive-operator valued measure (POVM) on A and $p_a = \text{Tr}[\rho_{AB} E_a]$ is the probability of outcome a .

a. Gaussian discord for harmonic oscillators

Originally proposed for qubits, the above definition of quantum discord has been generalized to Gaussian states for continuous-variable systems [32, 46] under the name of Gaussian discord D_G . This is obtained by restricting the optimization in Eq. (F2) to Gaussian POVM. As a consequence D_G provides in general only a lower bound for \mathcal{D} (namely, states with non zero values of D_G will certainly exhibit a certain amount of discord). For Gaussian states, yet, it is conjectured to be optimal, i.e. $D_G = \mathcal{D}$ [32, 46–48]. Gaussian discord is analytically computable for all two-mode Gaussian states (notably, all such states, except product states, have non-zero Gaussian discord).

The correlation matrix (see Sec. IV A) can be arranged in a (2×2) -block form as

$$C = \begin{pmatrix} C_1 & C_3 \\ C_3^\top & C_2 \end{pmatrix}. \quad (\text{F4})$$

From the correlation matrix C , five symplectic invariants [29] can be constructed

$$I_1 = 4 \text{Det}[C_1], \quad I_2 = 4 \text{Det}[C_2], \quad I_3 = 4 \text{Det}[C_3], \\ I_4 = 16 \text{Det}[C], \quad I_\Delta = I_1 + I_2 + 2I_3,$$

and two symplectic eigenvalues

$$\lambda_\pm = \sqrt{\frac{I_\Delta \pm \sqrt{I_\Delta^2 - 4I_4}}{2}}. \quad (\text{F5})$$

Gaussian discord can be defined in terms of these quantities (which are invariant under local unitary operations) as

$$D_G(B|A) = f(\sqrt{I_1}) - f(\lambda_-) - f(\lambda_+) + f(\sqrt{W}), \quad (\text{F6})$$

where

$$f(x) \equiv \left(\frac{x+1}{2}\right) \log_2 \left(\frac{x+1}{2}\right) - \left(\frac{x-1}{2}\right) \log_2 \left(\frac{x-1}{2}\right) \quad (\text{F7})$$

and

$$W = \begin{cases} \frac{2I_3^2 + (I_1 - 1)(I_4 - I_2) + 2|I_3|\sqrt{I_3^2 + (I_1 - 1)(I_4 - I_2)}}{(I_1 - 1)^2} & \text{if } (I_4 - I_2 I_1)^2 \leq (1 + I_1)I_3^2(I_2 + I_4) \\ \frac{I_2 I_1 - I_3^2 + I_4 - \sqrt{I_3^4 + (I_4 - I_2 I_1)^2 - 2I_3^2(I_4 + I_2 I_1)}}{2I_1} & \text{otherwise,} \end{cases} \quad (\text{F8})$$

The analogous quantity $D_G(A|B)$ can be computed by exchanging I_1 with I_2 in the above formulas and describes the correlations retrieved by measuring subsystem B first (instead of subsystem A). For the initial states considered in Section V, exchanging the role of the two subsystems has no effect, so that the two quantities coincide and we simply call them D_G .

b. Qubits

For a two-qubit system, the local measurement on system A is written as $\Pi_l^A(\theta, \phi) = |l\rangle_A \langle l| \otimes \mathbb{1}_B$ ($l = 1, 2$) with

$$|1\rangle = \cos\left(\frac{\theta}{2}\right) |e\rangle + e^{i\phi} \sin\left(\frac{\theta}{2}\right) |g\rangle, \quad (\text{F9})$$

$$|2\rangle = \sin\left(\frac{\theta}{2}\right) |e\rangle - e^{i\phi} \cos\left(\frac{\theta}{2}\right) |g\rangle \quad (\text{F10})$$

being orthogonal single-qubit states. The total amount of classical correlations [cf. (F3)] reads

$$\mathcal{C}(B|A) = \max_{\theta, \phi} \left[S(\rho_B) - \sum_l p_l S\left(\frac{\text{Tr}_A[\Pi_l^A(\theta, \phi)\rho\Pi_l^A(\theta, \phi)]}{p_l}\right) \right].$$

2. Entanglement

a. Harmonic oscillators

In Section V, we use *logarithmic negativity* for measuring entanglement of harmonic oscillators. It directly stems from the positive partial transpose (PPT) criterion [49] for discriminating entangled and separable states. A bipartite separable state can be written by definition as $\rho_{SEP} = \sum_i p_i \rho_A^{(i)} \otimes \rho_B^{(i)}$, with $\rho_A^{(i)}$, $\rho_B^{(i)}$ being states of the subsystems A and B respectively and p_i being probabilities. It's easy to see that its partial transpose with respect to one subsystem (say A) $\rho_{SEP}^{\top_A} = \sum_i p_i \rho_A^{(i)\top} \otimes \rho_B^{(i)}$ is still a valid density matrix and hence is positive definite. Conversely, a non positive partial transpose always indicates

the presence of entanglement. The logarithmic negativity quantifies how negative the partial transpose is.

For $1 \otimes 1$ -modes gaussian states the PPT criterion is both necessary and sufficient [50]. This also implies that the logarithmic negativity is a faithful measure of entanglement. In terms of correlation matrix C , partial transposition is equivalent to changing the sign of momenta for a subsystem (say A). The partial transpose C^{\top_A} is positive if and only if its symplectic eigenvalue $\tilde{\lambda}_-$ is greater than $1/2$ [29]. The symplectic eigenvalue $\tilde{\lambda}_-$ can be found, analogously to eq (F5), as

$$\tilde{\lambda}_- = \sqrt{\frac{\tilde{I}_\Delta - \sqrt{\tilde{I}_\Delta^2 - 4I_4}}{2}}, \quad (\text{F11})$$

where now $\tilde{I}_\Delta = I_1 + I_2 - 2I_3$ (note the change of sign due to partial transposition). The logarithmic negativity E_N is then defined as

$$E_N = \max\{0, -\log(2\tilde{\lambda}_-)\}. \quad (\text{F12})$$

Consistently $E_N > 0$ when $\tilde{\lambda}_- < 1/2$.

b. Qubits

The *concurrence* is a measure of entanglement of two-qubit states, which is given by

$$C(\rho) = \max(\lambda_1 - \lambda_2 - \lambda_3 - \lambda_4, 0), \quad (\text{F13})$$

where $\{\lambda_i\}$ are the square roots of the eigenvalues of matrix $M(\rho) = \rho(\hat{\sigma}_{1y}\hat{\sigma}_{2y})\rho^*(\hat{\sigma}_{1y}\hat{\sigma}_{2y})$ sorted in decreasing order while ρ^* is the complex conjugate of density matrix ρ . For two-qubit X states

$$\rho = \begin{pmatrix} a & 0 & 0 & w^* \\ 0 & b & z^* & 0 \\ 0 & z & c & 0 \\ w & 0 & 0 & d \end{pmatrix} \quad (\text{F14})$$

Eq. (F13) in this case becomes

$$C(\rho) = \max\left[2(|w| - \sqrt{bc}), 2(|z| - \sqrt{ad}), 0\right]. \quad (\text{F15})$$

For the initial states addressed in Section VI C we thus find

$$C[\rho(0)] = \max\left[\frac{1}{2} (|\rho_{23}(0)| + \xi_S^2 - 1), 0\right] = 0, \quad (\text{F16})$$

where we have taken into account Eq. (42) in the main text.